VILNIUS UNIVERSITY

CENTER FOR PHYSICAL SCIENCES AND TECHNOLOGY

EGLĖ GABRYTĖ

APPLICATIONS OF FEMTOSECOND LASER PULSES IN REFRACTIVE EYE SURGERY

Summary of doctoral dissertation

Physical sciences, Physics (02P)

Vilnius, 2015

Dissertation was prepared at Vilnius University in 2011–2015

Scientific supervisor – dr. Mikas Vengris (Vilnius University, Physical sciences, Physics – 02P)

Dissertation will be defended in the Council of Physics of Vilnius University:

Chairman – prof. habil. dr. Valerijus Smilgevičius (Vilnius University, Physical sciences, Physics – 02P)

Members:
prof. dr. Roaldas Gadonas (Vilnius University, Physical sciences, Physics – 02P)
dr. Martynas Beresna (University of Southampton, United Kingdom, Physical sciences, Physics – 02P)
dr. Gediminas Račiukaitis (Center for Physical Sciences and Technology, Physical sciences, Physics – 02P)
dr. Saulius Bagdonas (Vilnius University, Biomedical sciences, Biophysics – 02B)

The official defence of the dissertation will be held on 25th of September, 2015, in auditorium 306 at the Laser Research Center of Vilnius University, at 14 p.m.

Address: Saulėtekio 10, 10223 Vilnius, Lithuania

Summary of the dissertation was distributed on the 25 of August, 2015.
The dissertation is available for preview in the libraries of Vilnius University and of Center for Physical Sciences and Technology and on the website: *www.vu.lt/lt/naujienos/ivykiu-kalendorius*

VILNIAUS UNIVERSITETAS

FIZINIŲ IR TECHNOLOGIJOS MOKSLŲ CENTRAS

EGLĖ GABRYTĖ

FEMTOSEKUNDINIŲ LAZERIO IMPULSŲ TAIKYMAS REFRAKCINEI CHIRURGIJAI

Daktaro disertacijos santrauka

Fiziniai mokslai, fizika (02P)

Vilnius, 2015

Disertacija rengta 2011–2015 metais Vilniaus universitete

Mokslinis vadovas – dr. Mikas Vengris (Vilniaus universitetas, fiziniai mokslai, fizika – 02P)

Disertacija ginama Vilniaus universiteto Fizikos mokslo krypties taryboje:

Pirmininkas – prof. habil. dr. Valerijus Smilgevičius (Vilniaus universitetas, fiziniai mokslai, fizika – 02P)

Nariai:
prof. dr. Roaldas Gadonas (Vilniaus universitetas, fiziniai mokslai, fizika – 02P)
dr. Martynas Beresna (Southamptono universitetas, Jungtinė Karalystė, fiziniai mokslai, fizika – 02P)
dr. Gediminas Račiukaitis (Fizinių ir technologijos mokslų centras, fiziniai mokslai, fizika – 02P)
dr. Saulius Bagdonas (Vilniaus universitetas, biomedicinos mokslai, biofizika – 02B)

Disertacija bus ginama viešame Fizikos mokslo krypties tarybos posėdyje 2015 m. rugsėjo mėn. 25 d. 14 val. Vilniaus universiteto Lazerinių tyrimų centre, 306 auditorijoje.

Adresas: Saulėtekio al. 10, Vilnius Lietuva

Disertacijos santrauka išsiuntinėta 2015 m. rugpjūčio mėn. 25 d.
Disertaciją galima peržiūrėti Vilniaus universiteto ir Fizinių ir technologijos mokslų centro bibliotekose ir Vilniaus universiteto interneto svetainėje adresu: *www.vu.lt/lt/naujienos/ivykiu-kalendorius*

Contents

List of abbreviations

ArF – argon fluoride

BBO – βBaB_2O_4, beta barium borate

CW – continuous wave

DNA – deoxyribonucleic acid

ex vivo – [Latin] outside the living body

FHG – fourth-harmonic generator

FWHM – full width at half maximum

in vivo – [Latin] within a living organism

in vitro – [Latin] in an artificial environment outside a living organism

LASIK – laser-assisted *in situ* keratomileusis

NA – numerical aperture

nIR – near-infrared

PMMA – polymethyl methacrylate

PRK – photorefractive keratectomy

PTK – phototherapeutic keratectomy

SmILE – small incision lenticule extraction

TransPRK – transepithelial photorefractive keratectomy

Yb:KGW – ytterbium-doped potassium gadolinium tungstate

UV – ultraviolet

Chapter 1

Introduction

Refractive errors—myopia (nearsightedness), hyperopia (farsightedness), astigmatism and presbyopia (loss of the near vision with age)—negatively influence the quality of human life. Myopia is an increasingly widespread condition around the world [1–7], especially in the east Asia [1,8]. The higher prevalence of myopia seems to be associated with the increasing educational pressure combined with lifestyle changes, which result in the reduced time children spend outside [1,2]. Effective reduction of the visual impairment is available with optical correction by spectacles, contact lenses, and refractive surgery.

The most popular surgical procedure for treatment of refractive errors is the laser-assisted *in situ* keratomileusis (LASIK) [9]. During the LASIK procedure a thin corneal flap is created using a surgical knife (microkeratome) or using the femtosecond near-infrared (nIR) laser pulses. Then the corneal flap is opened and the corneal stroma is reshaped using the nanosecond ultraviolet (UV) laser pulses. After that the corneal flap is replaced and the optical quality of the eye surface is restored. It was demonstrated, that if the LASIK flap is created using the femtosecond laser pulses (in this case the procedure is called Femto-LASIK [10]), the results of the surgery are better than if the flap is created using a microkeratome [11–16].

The main disadvantage of this procedure is that it requires two different laser sources. The patient has to be transferred from one laser system to the other in the middle of the surgery, and the surgeon must be able to master both laser systems (often of different manufacturers). Special requirements for the operating room must also be satisfied and, of course, two laser systems are twice as expensive as a single one. Therefore, there is a need for a single laser system, which would be able to perform the entire refractive correction procedure. Indeed, myopia correction can be performed using only femtosecond nIR pulses in SmILE (small incision lenticule extraction)

all-femtosecond procedure [17], where the lens-shaped cutting inside the cornea (a so-called lenticule) is created and then mechanically removed. However, it is rather limited: the procedure is not suitable for hyperopia correction [18], for small refractive changes, and retreatment is possible only with the UV laser [19]. During the previous decade the femtosecond solid-state laser technology has been intensively developed and today it is possible to have a single femtosecond laser source, emitting both nIR an UV pulses.

Main goal and tasks of the research work

The main goal of this work is to explore the possibility to replace two different laser systems (UV nanosecond and nIR femtosecond), that are currently used for the refractive corneal surgery, with a single Yb:KGW femtosecond nIR laser equipped with the UV harmonic generator.

The main tasks of this work:

1. To design a fifth-harmonic generator (205 nm) of the Yb:KGW femtosecond laser and develop the ablation algorithm for high-speed correction of myopia, ensuring the minimal thermal collateral damage to the superficial layers of the cornea.

2. To optimize the parameters of the laser system and to assess the ablation rate of *ex vivo* and *in vivo* corneal stroma, quality of the ablated corneal surface, and to evaluate the healing course and pathological changes of *in vivo* cornea after the femtosecond UV ablation. To compare the obtained characteristics with those of the conventional refractive surgery using excimer ArF laser system.

3. To utilize femtosecond nIR pulses of the Yb:KGW laser in creation of the corneal flap in the LASIK procedure as well as in performing the whole SmILE procedure. To explore, how the surface quality, predictability and repeatability of the femtosecond cutting procedure results depends on the beam focusing optics and the laser radiation parameters.

4. To assess the cytotoxic and genotoxic impact of the femtosecond UV pulses on cells *in vitro* and compare it with the impact of the other UV sources.

Statements of the thesis

1. The rate, at which the radiation of the high repetition rate femtosecond UV harmonic generator can be manipulated, is limited by the absorption of UV pulses in nonlinear optical crystals. This rate can be increased by a few orders of magnitude by implementing the adaptive manipulation of the tuning angle of the nonlinear crystal.

2. Using the fundamental nIR radiation of the Yb:KGW solid-state laser, the corneal LASIK flap is created precisely and reproducibly; the duration of the procedure is comparable to the commercial laser systems.

3. Performance of the femtosecond Yb:KGW solid-state system is comparable to the conventional excimer ArF laser systems with respect to the ablation speed and the surface quality of the corneal stroma.

4. The cytotoxic and genotoxic impact of the UV radiation on cells depends on the wavelength of the UV source rather than on the pulse duration. The genotoxic impact of the femtosecond 205 nm pulses does not exceed the one of the nanosecond UV pulses, that are used for ophthalmic procedures.

5. Most of modern ophthalmic laser procedures can be performed using the single solid-state Yb:KGW femtosecond laser system equipped with the fifth-harmonic generator.

Novelty and relevance of the results

It is known, that thermal effects in the nonlinear optical UV harmonic generators reduce the conversion efficiency, decrease the quality of the beam characteristics and change the phase matching conditions [20, 21]. When long (nanosecond or picosecond) pulses are converted, the thermal effects inside the nonlinear crystal can be reduced by using the different cooling techniques [22–24]. However, they are not effective when the high repetition rate femtosecond pulses are converted into UV region. In this work, a new method, employing the adaptive manipulation of the tuning angle of the nonlinear crystal, is presented. We propose, that this method is suitable for many different micromachining applications, where the processing speed is of a high importance.

The solid-state nanosecond lasers with the UV converters are used for the corneal stroma reshaping as the alternative for the excimer ArF lasers

since 2004 [25, 26]. Although the results of the corneal ablation using the solid-state nanosecond laser systems meet the requirements regarding safety and predictability [27–29], it is difficult for these systems to compete with the older and well-established excimer laser technology. To our knowledge, here reported corneal ablation using femtosecond 205 nm pulses was performed for the first time. The results of the femtosecond corneal ablation were identical to the nanosecond ArF excimer laser in terms of the ablated corneal surface quality and healing response. Femtosecond pulses are known to produce less thermal collateral damage than nanosecond pulses, therefore thermal impact to the cornea should be reduced due to the shorter pulses.

In this work, we demonstrate the possibility to perform the whole Femto-LASIK procedure using a single solid-state Yb:KGW femtosecond laser system. To our knowledge, this was done for the first time, although announcement (but not demonstration) of such all-solid-state system from one manufacturer was made without any related information in the scientific literature [30]. Our solid-state laser system is capable to perform more than Femto-LASIK. It can be used to correct refractive errors only with femtosecond nIR pulses, perform transepithelial ablation with UV pulses, and has potential to be used for treatment of presbyopia or even cataract.

It is known, that shorter UV wavelengths (193–213 nm) cause less genotoxic effects in the living cells than the longer wavelengths (240–270 nm) [31–33]. However, the dependence of the DNA damage on the duration of UV pulses (especially femtosecond pulses) has never been investigated. We assessed and compared the cytotoxic and genotoxic impact of the femtosecond UV pulses and of the other UV sources. We found that in the UV region the amount of DNA damage is determined by the wavelength of the light and not the duration of the pulses. We report, that femtosecond 205 nm pulses have the strongest cytotoxic effect and low genotoxic impact, therefore, the possibility for a cell, irradiated with 205 nm femtosecond pulses, to mutate is smaller compared to the other investigated UV sources.

Approbation of the results

The results were presented in 6 scientific papers:

1. E. Gabryte, S. Sobutas, M. Vengris, R. Danielius, Control of thermal effects in fast-switching femtosecond UV laser system, Appl. Phys. B **120**(1), 31-39 (2015).

2. E. Danieliene, E. Gabryte, M. Vengris, O. Ruksenas, A. Gutauskas,

V. Morkunas, R. Danielius, High-speed photorefractive keratectomy with femtosecond ultraviolet pulses, J. Biomed. Opt. **20**(5), 051037 (2015).

3. E. Danieliene, E. Gabryte, R. Danielius, M. Vengris, A. Vaiceliunaite, V. Morkunas, O. Ruksenas, Corneal stromal ablation with femtosecond ultraviolet pulses in rabbits, J. Cataract Refract. Surg. **39**, 258-267 (2013).

4. E. Gabryte, E. Danieliene, A. Vaiceliunaite, O. Ruksenas, M. Vengris, R. Danielius, All-femtosecond laser-assisted in situ keratomileusis, Proc. SPIE **8567**, Ophthalmic Technologies XXIII, 85671S-85671D-7 (2013).

5. V. Morkunas, O. Ruksenas, M. Vengris, E. Gabryte, E. Danieliene, R. Danielius, DNA damage in bone marrow cells induced by ultraviolet femtosecond laser irradiation, Photomed. Laser Surg. **29**(4), 239-244 (2011).

6. M. Vengris, E. Gabryte, A. Aleknavicius, M. Barkauskas, O. Ruksenas, A. Vaiceliunaite, R. Danielius, Corneal shaping and ablation of transparent media by femtosecond pulses in deep ultraviolet range, J. Cataract Refract. Surg. **36**(9), 1579-1587 (2010).

The results were presented at the conferences:

1. S. Sobutas, E. Gabryte, R. Danielius, Femtosekundinių ultravioletinių impulsų generavimas: šiluminiai reiškiniai ir jų valdymas, 41-oji Lietuvos nacionalinė fizikos konferencija (Vilnius, Lithuania, 2015).

2. S. Sobutas, E. Gabryte, Control of thermal effects in high harmonics generator of solid-state femtosecond laser, Open readings 2015 (Vilnius, Lithuania, 2015).

3. E. Gabryte, E. Danieliene, A. Vaiceliunaite, O. Ruksenas, M. Vengris, R. Danielius, High-speed transepithelial corneal ablation using a solid-state femtosecond laser based system, Laser Applications in Life Sciences (Ulm, Germany, 2014).

4. E. Gabryte, M. Vengris, R. Danielius, Thermal effects in the fourth harmonic generator of femtosecond Yb:KGW laser, Open readings 2014 (Vilnius, Lithuania, 2014).

5. E. Gabryte, E. Danieliene, A. Vaiceliunaite, O. Ruksenas, M. Vengris, R. Danielius, Universali femtosekundinė lazerinė sistema regos ydų korekcijai, Ketvirtoji jaunųjų mokslininkų konferencija „Fizinių ir technologijos mokslų tarpdalykiniai tyrimai“ (Vilnius, Lithuania, 2014).

6. E. Gabryte, E. Danieliene, A. Vaiceliunaite, O. Ruksenas, M. Vengris, R. Danielius, Complete LASIK procedure using a solid-state femtosecond laser based system, European Conferences on Biomedical Optics (Munich, Germany, 2013).

7. E. Gabryte, E. Danieliene, A. Vaiceliunaite, O. Ruksenas, M. Vengris, R. Danielius, Lazerinė refrakcinė regos korekcija LASIK naudojant vien tik femtosekundinę kietakūnę lazerinę sistemą, 40-oji Lietuvos nacionalinė fizikos konferencija (Vilnius, Lithuania, 2013).

8. E. Gabryte, E. Danieliene, A. Vaiceliunaite, O. Ruksenas, M. Vengris, R. Danielius, All-femtosecond laser-assisted in situ keratomileusis, Photonics West (San Francisco, USA, 2013)

9. E. Gabryte, M. Vengris, R. Danielius, E. Danieliene, A. Vaiceliunaite, Ragenos lopo formavimas femtosekundinio kietakūnio Yb:KGW lazerio impulsais, 39-oji Lietuvos nacionalinė fizikos konferencija (Vilnius, Lithuania, 2011).

10. E. Gabryte, M. Vengris, R. Danielius, O. Ruksenas, A. Vaiceliunaite, E. Danieliene, Femtosecond solid-state UV laser system for the refractive eye surgery, Open readings 2011 (Vilnius, Lithuania, 2011).

11. E. Gabryte, M. Vengris, R. Danielius, O. Ruksenas, A. Vaiceliunaite, Efficient ablation of ex vivo cornea using the fifth harmonic of femtosecond Yb:KGW laser, Open readings 2010 (Vilnius, Lithuania, 2010).

12. E. Danieliene, R. Danielius, E. Gabryte, O. Ruksenas, A. Vaiceliunaite, M. Vengris, Corneal stromal ablation by femtosecond UV pulses: in vivo study, The World Ophthalmology Congress (Berlin, Germany, 2010).

13. E. Danieliene, R. Danielius, E. Gabryte, V. Morkunas, O. Ruksenas, A. Vaiceliunaite, M. Vengris, Ablation of rabbit cornea by femtosecond ultraviolet pulses, The XIII Forum Ophthalmologicum Balticum (Vilnius, Lithuania, 2010).

14. E. Gabryte, M. Vengris, R. Danielius, O. Ruksenas, A. Vaiceliunaite, Efficient ablation of ex vivo cornea using the fifth harmonic of fem-

tosecond Yb:KGW laser, Biomedical Engineering (Vilnius, Lithuania, 2009).

15. E. Gabryte, A. Aleknavicius, R. Danielius, M. Vengris, Efficient ablation of ex vivo cornea by the fifth harmonic of femtosecond Yb:KGW laser, Northern Optics (Vilnius, Lithuania, 2009).

16. E. Gabryte, M. Vengris, A. Aleknavicius, R. Danielius, Efektyvus antrosios, ketvirtosios ir penktosios harmonikos generatorius femtosekundiniam Yb:KGW lazeriui, 38-oji Lietuvos nacionalinė fizikos konferencija (Vilnius, Lithuania, 2009).

17. E. Gabryte, M. Vengris, A. Aleknavicius, R. Danielius, Corneal shaping by femtosecond UV laser pulses, 38-oji Lietuvos nacionalinė fizikos konferencija (Vilnius, Lithuania, 2009).

Chapter 2

Refractive laser surgery

The main purpose of the refractive laser surgery is to adjust the refractive properties of a human's eye and free the patient from wearing glasses or contact lenses. In a myopic eye, the refractive power of the cornea and the lens is too strong in relation to the length of the eyeball. Thus, in the refractive eye surgery the corneal surface has to be flattened in the central area in order to reduce the refractive power there. In the cornea of a hyperopic eye, the refractive power is too low and the surface must be steepened by removing most of the tissue at the edge of the cornea. By shaping the corneal surface to a certain degree on different axis, refractive errors like astigmatism can also be corrected.

Refractive laser surgery was proposed in 1983 [34]. Today it is a routine surgical procedure, shared by two different methods: photorefractive keratectomy (PRK) and LASIK.

In the PRK procedure, the epithelium of the eye is first mechanically or chemically removed. After that, the refractive change of the corneal stroma is created by ablation using nanosecond UV pulses (193 nm wavelength), provided by the ArF excimer laser. According to the amount of the refractive error, some 10 μm or as much as 100 μm of the superficial layer of the cornea is removed. In a few days after the procedure, the epithelium layer regrows and the optical quality of the eye surface returns.

The course of LASIK procedure is presented in Fig. 2.1. During the LASIK procedure, a thin layer of the cornea is partially separated by a surgical knife (microkeratome) or using tightly focused femtosecond nIR laser pulses (the procedure is then referred to as Femto-LASIK, see Fig. 2.1, a). After opening the corneal flap (Fig. 2.1, b), corneal stroma is ablated by the UV laser pulses to correct the refractive power of the eye (Fig. 2.1, c). At the end, the corneal flap is replaced (Fig. 2.1, d). The LASIK procedure avoids the anterior stromal haze and pain that are frequently associated

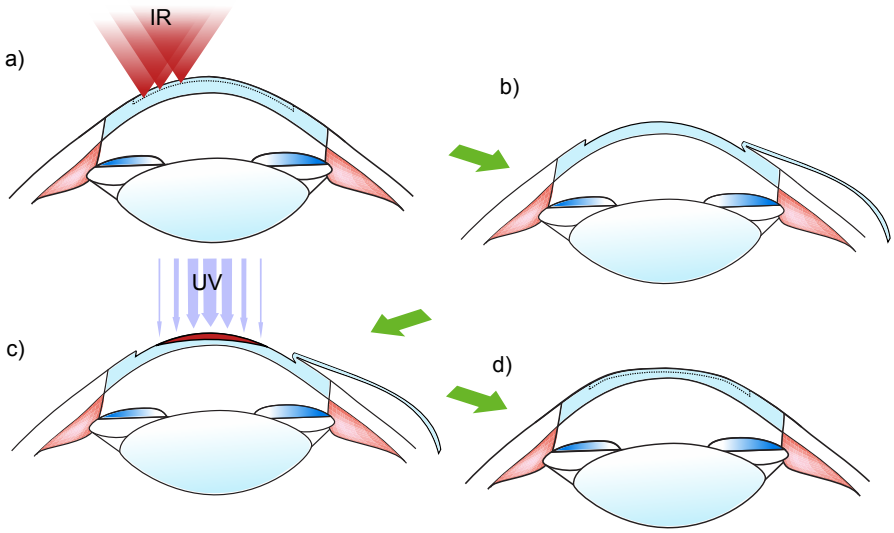

Figure 2.1: Femto-LASIK procedure: corneal flap creation using femtosecond nIR pulses (a), opening of the corneal flap (b), reshaping of the corneal stroma with UV laser pulses (c) and closing of the corneal flap (d).

with PRK [35–37]. This result is achieved because the laser is applied only within the corneal substance, therefore avoiding damage to the corneal epithelium. With LASIK, the epithelium remains almost entirely intact; thus the nerve endings stay protected, there is minimal pain during the recovery, and there is a lower risk of infection and scarring [38].

As the accuracy and the predictability of the femtosecond lasers has increased, new procedures for modifying the corneal shape became possible. These include SmILE and FLEx (femtosecond lenticule extraction) [17, 39]. In these procedures, pulses of the femtosecond laser are used to cut a lenticule within the corneal stroma corresponding to the refractive correction required. During the FLEx procedure the lenticule is removed after the corneal flap is created and opened. In the SmILE procedure the lenticule is extracted through a small tunnel incision. The proposed advantage of SmILE is that the structural integrity of the cornea is maintained and the complications associated with flaps are avoided since no flap is cut. However, this technique has only been used to correct myopia so far and the retreatment is possible only with the UV laser [19].

Chapter 3

Control of thermal effects in fast-switching femtosecond UV laser system

Femtosecond laser systems are becoming essential tools in various areas of material processing, medicine and scientific research. In order to tailor the wavelength of radiation to the absorptivity of materials being processed, UV harmonic generators are often employed. At high average powers and high repetition rates the long warm-up time of harmonic generators, caused by linear and two-photon absorption (TPA) in nonlinear crystals [20,21,40–42], can be a serious obstacle for efficient and fast processing. To increase the speed and reduce the cost of technological processes, new methods are required to speed-up the settling of the output power when the harmonic generators are switched on after a longer idle period. We have investigated the fourth-harmonic generator (FHG) of a high repetition rate femtosecond laser and studied properties of the output radiation in order to optimize its fast-switching capabilities. Theoretical modeling of thermal effects in the nonlinear crystal allowed us to explain temporal dependencies of the temperature and the output power after switching the laser on. Based on these results, we were able to optimize the trajectory of the nonlinear crystal rotation following the system start-up and, consequentially, reduced the switching-on time from tens of seconds to 50 milliseconds without any negative effect on the output.

3.1 Experimental setup

The driving laser system was a solid-state femtosecond Yb:KGW laser "Pharos" ("Light Conversion", Lithuania) lasing in the near-infrared (λ = 1026 nm) and operating at 50 kHz pulse repetition rate with an average power of 3 W and the pulse duration of 280 fs. The laser featured a near-Gaussian beam profile ($M^2 = 1.1$) with a diameter of 1.5 mm at the $1/e^2$ intensity level.

Femtosecond pulses in the UV range were obtained by generating the fourth laser harmonic as shown in Fig. 3.1; the fundamental laser radiation was converted to the second (513 nm) and, subsequently, to the fourth (257 nm) harmonic using β-barium borate (BBO) nonlinear optical crystals $NC_{2\omega}$ (2 mm length, cut at $\theta_{PM2\omega} = 23.5°$) and $NC_{4\omega}$ (0.7 mm length, cut at $\theta_{PM4\omega} = 50.4°$), respectively. The phase matching angle of the $NC_{4\omega}$ crystal was adjusted using a stepper motor-driven rotation stage MRS. The mirrors M_2 and M_3 were used for the separation of the fourth-harmonic radiation.

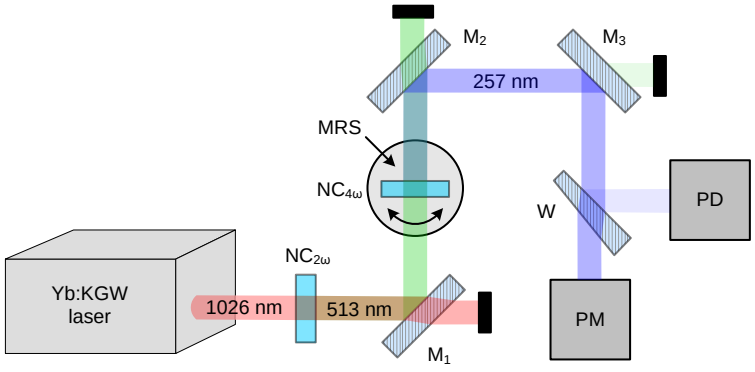

Figure 3.1: The optical setup for the measurement of temporal output characteristics of the femtosecond FHG. M_1–M_3 are mirrors, $NC_{2\omega}$, $NC_{4\omega}$ – nonlinear optical crystals, W – wedge, MRS – motorized rotation stage, PD – photodetector, PM – power meter.

The resulting pulses at 257 nm were detected by the fast UV-sensitive Si photodetector (PD) "DET10A" ("Thorlabs", USA). The response function of the detector was linearized and calibrated using power meter (PM) "Ophir Nova II", equipped with thermal power sensor "30A-BB-18" ("Ophir Optronics", Israel). The temperature distribution on the surfaces of nonlinear crystal was recorded using an infrared camera "Thermacam S65" ("FLIR Systems", USA). In order to obtain the actual temperature correctly, the emissivity value of 0.82 of the back-surface of the fourth-harmonic BBO crystal (anti-reflective coated) was used. This value was estimated from a separate thermal picture of the crystal homogeneously heated to a known

temperature.

3.2 Temporal switch-on dynamics

To demonstrate the influence of the initial crystal phase matching angle and the heat production on the frequency conversion process, the switch-on/switch-off dynamics of the FHG output power and the concomitant growth/drop of the $NC_{4\omega}$ crystal temperature were measured. It must be noted that TPA-induced heating is negligible for the $NC_{2\omega}$ crystal, because the combined energy of two 513 nm photons is lower than the bandgap energy of the BBO crystal [43]. Therefore, by measuring the fourth-harmonic output power we observed mainly the effects pertaining to the $NC_{4\omega}$ crystal.

Temporal dynamics of the FHG output power and crystal temperature after switching the driving laser on are shown in Fig. 3.2. Solid lines correspond to the turn-on dynamics measured at different angular detuning $\Delta\theta \equiv \theta - \theta_0$ of the nonlinear crystal $NC_{4\omega}$. The angular detuning $\Delta\theta$ is defined as the deviation of the crystal angle θ from the reference angle θ_0 at which the highest FHG output power (760 mW) was observed when the harmonic generator was optimized under the continuous operation of the driving laser. To simplify the further mathematical expressions, the experimentally observed crystal angles were recalculated into the internal angle between the light propagation direction and the principal optical axis of the nonlinear crystal (in the same manner as the phase matching angle is defined). At $\Delta\theta = 0$, the highest temperature (62 °C) of the crystal surface at the center of the laser beam was also observed. However, it should be noted, that the angular detuning $\Delta\theta$ differs from the angular phase mismatch $\Delta\theta_{\mathrm{PM}}(T) \equiv \theta - \theta_{\mathrm{PM}}(T)$, because the optimal phase matching condition across the laser beam depends on the spatial distribution of the crystal temperature (which, in turn, depends on the time passed after switching-on of the driving laser system).

To explain the measured temporal dynamics of temperature and the FHG output power, a theoretical model of the fourth-harmonic generation concomitant with the crystal heating was developed. The heat generation and dissipation within the crystal was described using a two-temperature model. We virtually divided the crystal into two zones, denoted as the center and the periphery. The center was considered as directly affected by the absorption of the fourth-harmonic radiation, whereas the surrounding periphery was considered to be a strongly coupled thermal energy acceptor that takes

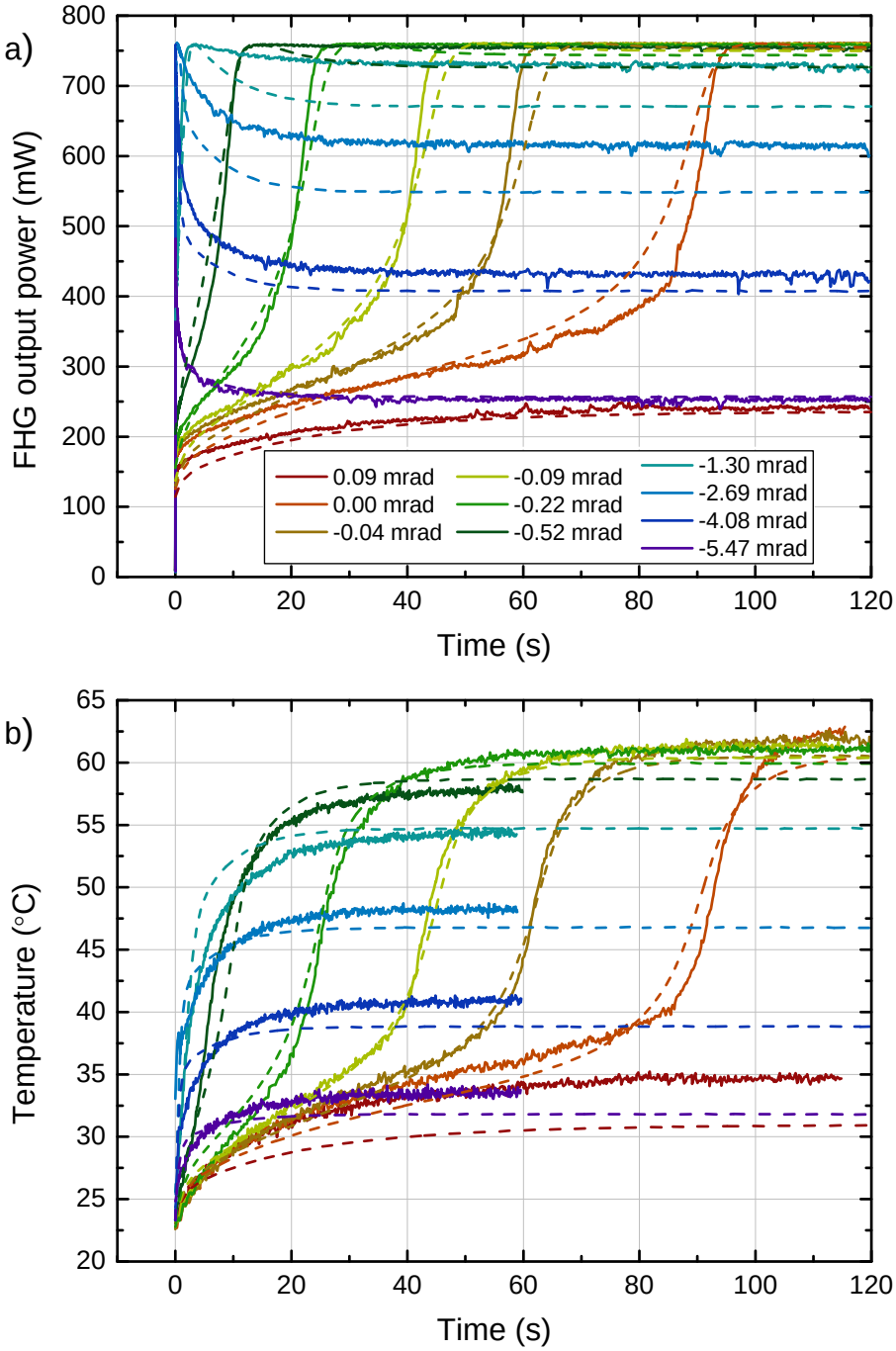

Figure 3.2: Measured (solid lines) and simulated (dashed lines) temporal dynamics of the fourth-harmonic power (a) and nonlinear crystal temperature (b) at different angular detuning values $\Delta\theta$.

the heat away from the center and transfers it to the environment at a slower rate. The heat balance equations for the center (temperature T) and the periphery of the crystal can then be written down as follows:

$$\rho c_{\mathrm{p}} \frac{\mathrm{d}T}{\mathrm{d}t} = \tau f \left(\alpha I_{\mathrm{IV}} (\theta, T) + \beta I_{\mathrm{IV}}^2 (\theta, T) \right) - h_1 (T - T_{\mathrm{p}}) , \tag{3.1}$$

$$\rho c_{\mathrm{p}} \frac{\mathrm{d}T_{\mathrm{p}}}{\mathrm{d}t} = \frac{h_1}{\xi} (T - T_{\mathrm{p}}) - h_2 (T_{\mathrm{p}} - T_0) . \tag{3.2}$$

Here T_{p} and T_0 are the temperatures of the periphery of the crystal and the environment, respectively; ξ – the effective ratio of volumes of the periphery and the center, α and β are the relative linear absorption and the TPA coefficients, respectively, ρ is the mass density of the BBO crystal, c_{p} – specific heat capacity, τ – pulse duration and f – pulse repetition rate. Coefficients $h_1 = \frac{c_{\mathrm{p}}\rho}{\tau_1}$ and $h_2 = \frac{c_{\mathrm{p}}\rho}{\tau_2}$ are heat transfer rates from the center to the periphery and from the periphery to the environment, respectively. The FHG output intensity I_{IV} was approximated as Gaussian function of the angular detuning:

$$I_{\mathrm{IV}} (\theta, T) = \eta I_{\mathrm{II}} \exp \left(- \frac{4 \ln 2 (\theta - \theta_{\mathrm{PM}}(T))^2}{\Delta\theta_{\mathrm{BW}}^2} \right) , \tag{3.3}$$

I_{II} – the average intensity of the second-harmonic radiation, $\Delta\theta_{\mathrm{BW}}$ – angular phase matching bandwidth, and $\eta = 0.39$ – the measured conversion efficiency at the optimal phase matching. The phase matching angle is a function of the temperature, $\theta_{\mathrm{PM}}(T) = \theta_{\mathrm{PM}}(T_0) + \chi(T - T_0)$, and it is implicitly time dependent, because the temperature of the center T is a function of time.

The system of differential equations (3.1) and (3.2) was numerically solved using the fourth-order Runge–Kutta method; the Nelder–Mead simplex nonlinear optimization method [44] was used to find the best set of the free parameter values (α, β, ξ and χ) to fit the experimental dynamics of temperature and the FHG output power. The simulated dependencies of the FHG output power and the crystal temperature for different angular detuning values are plotted in Fig. 3.2 by dashed lines.

3.3 Motorized control of the crystal angle

The results presented above show that the thermal effects in the nonlinear fourth-harmonic generation crystal cause slow variations of the output power. Such a long warm-up time limits the practical application of the UV

harmonic generators of the high-power femtosecond lasers. To manage these side effects and to minimize the warm-up duration, the motorized control of the crystal angle was employed.

The basic idea of the motorized control of the crystal is to rotate it according to some time-dependent function of the angular detuning optimized to decrease the warm-up time as much as possible. Since the temperature dynamics of the crystal after switching the laser radiation off was well approximated by the two-exponential decay, we inferred, that the optimal function of the crystal rotation may also be a two-exponential decay function of time:

$$\Delta\theta(t) = A\mathrm{e}^{-\frac{t}{\tau_A}} + B\mathrm{e}^{-\frac{t}{\tau_B}}. \tag{3.4}$$

To optimize the amplitudes A and B and time constants τ_A and τ_B, we utilized the theoretical model described above. We added time-dependent rotation into Eq. (3.3) by replacing θ with $\theta_0 + \Delta\theta(t)$ and set the initial conditions of differential equations (3.1) and (3.2) representing system's equilibrium state at the room temperature: $T(0) = T_0(0) = T_\mathrm{p}(0) = 23.3\,^\circ\mathrm{C}$. The initial angular detuning corresponding to the phase matching condition at room temperature was found to be $\Delta\theta(0) = \theta(0) - \theta_0 = -3.56\,\mathrm{mrad}$. Nonlinear optimization of solutions of the differential equations was performed to minimize the time needed to achieve constant output power of $P_\mathrm{max} = 760\,\mathrm{mW}$. The best fitting parameters were found to be: amplitudes $A = -1.96\,\mathrm{mrad}$ and $B = -1.60\,\mathrm{mrad}$, and time constants $\tau_A = 0.93\,\mathrm{s}$ and $\tau_B = 10.00\,\mathrm{s}$. Theoretically optimized trajectory (shown in Fig. 3.3, b by red line) was directly applied for mechanical crystal angle manipulation and the FHG warm-up time was significantly reduced from $\sim 100\,\mathrm{s}$ to $\sim 2\,\mathrm{s}$ (see Fig. 3.3, a, red line).

The measured dynamics of the FHG output power revealed additional very fast processes, which were not accounted for in our theoretical model. During the first $\sim 70\,\mathrm{ms}$ after turning the laser radiation on, an instantaneous drop of the output power by $\sim 90\,\mathrm{mW}$ followed by a slow recovery in $\sim 2\,\mathrm{s}$ was observed (see inset in Fig. 3.3, a). The fast power decrease could be related with the formation and equilibration of thermal gradients along and/or across the beam propagation direction in the crystal. Additionally, to enhance the start-up characteristics as well as reduce the duration of motorized control, the amplitude A and the offset value were adjusted experimentally, keeping other parameters B, τ_A and τ_B fixed at their values obtained from the simulations. Almost perfectly steep rising

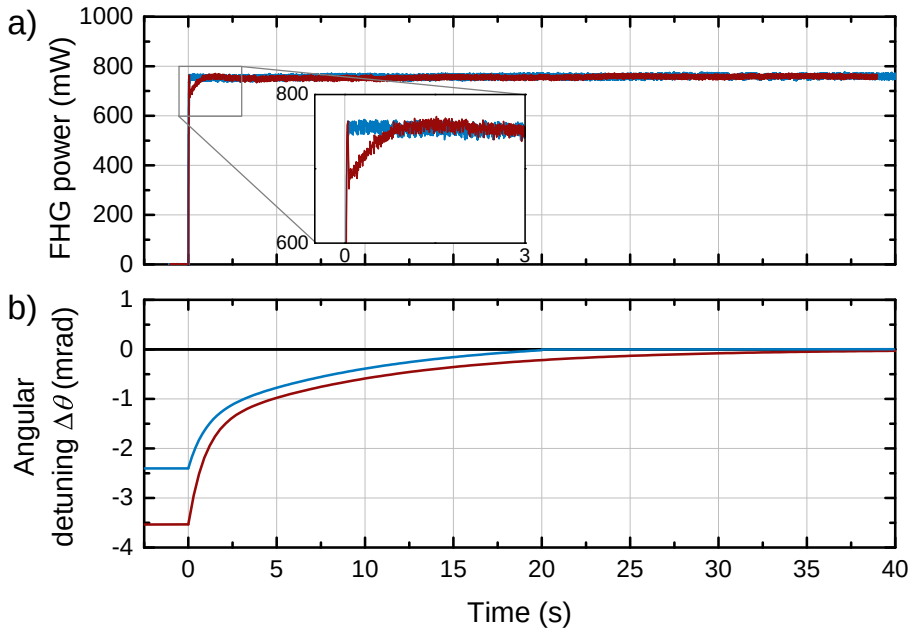

Figure 3.3: Time dependence of a) the FHG output power and b) angular detuning $\Delta\theta(t)$ obtained using optimized parameters from simulations (red lines) and after additional experimental adjustment (blue lines).

front of the switched-on power was achieved after reducing the amplitude A to -1 mrad and adding an offset value of 0.2 mrad. The best results of the motorized control of the crystal angle are presented in Fig. 3.3 by the blue lines. The highest UV power value is reached within 50 ms after turning the laser radiation on, and the overall duration of the motorized crystal control is 20 s.

Chapter 4

Corneal ablation using femtosecond UV pulses

Our first ablation experiments on model materials, such as gelatine, polymethyl methacrylate (PMMA) and *ex vivo* porcine eyes, have shown that 205 nm femtosecond laser system is capable to perform highly accurate and predictable surface ablation [45]. *In vivo* experiments on rabbits revealed that corneal healing response after femtosecond PRK procedure was similar to that after conventional PRK procedure using commercial excimer ArF laser system [46]. However, these experiments were performed with a low ablation rate (3.7 D/s). To investigate the healing response of the rabbit cornea after high-speed femtosecond ablation, we performed transepithelial photorefractive keratectomy (TransPRK). To increase the ablation rate of the corneal stroma, we have modified the laser system that was previously described in detail [45, 46].

The femtosecond UV pulses for corneal ablation was obtained by generating the fifth-harmonic of Yb:KGW laser pulses. The optical setup for generation of femtosecond UV (205 nm) pulses is presented in Fig. 4.1. The laser beam was controlled by using galvanometer mirror scanners "hurrySCAN II7" with RTC®5 PCI control board ("Scanlab", Germany).

The laser system operated at a 50 kHz pulse repetition rate, the pulse duration was $280 \pm 10\,\mathrm{fs}$ and the average power of the fundamental nIR radiation was 5 W. The overall conversion efficiency to the fifth-harmonic was 9.4 % (470 mW). UV pulse generator was equipped with a beam shaper to achieve a near second order super-Gaussian beam profile at the corneal surface. The beam diameter at the $1/e^2$ intensity level was estimated to be $115 \pm 5\,\mu\mathrm{m}$. Assuming the super-Gaussian intensity distribution, the peak fluence with these laser settings was $135 \pm 5\,\mathrm{mJ/cm^2}$.

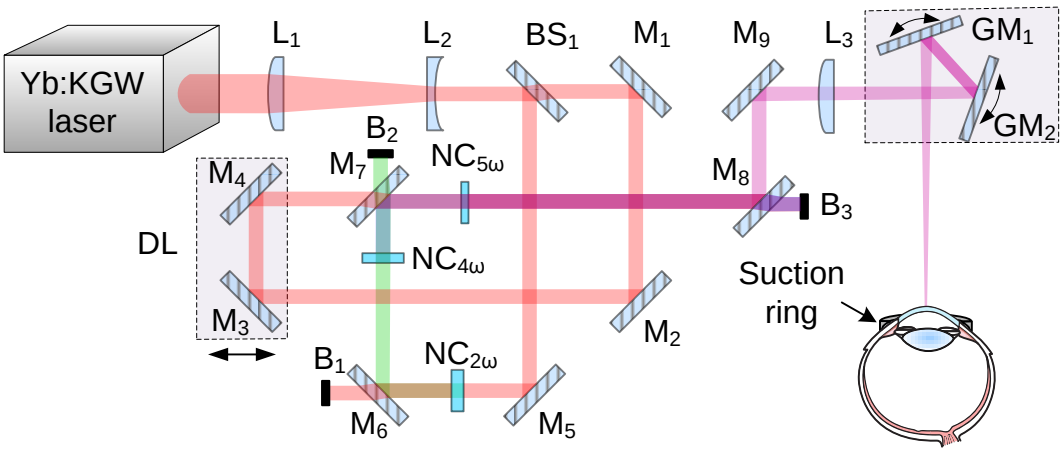

Figure 4.1: The layout of the fifth-harmonic generator for corneal ablation. L_1–L_3 – lenses, M_1–M_9 – mirrors, BS_1 – beam splitter, $NC_{2\omega}$, $NC_{4\omega}$, $NC_{5\omega}$ – nonlinear BBO crystals, DL – delay line, GM_1, GM_2 – galvanometer mirrors, B_1–B_3– beam blocks.

To evaluate the predictability and reproducibility of high-speed femtosecond PRK procedure, we performed the ablation experiments in rabbits.[1] Non-stop myopic TransPRK of $\sim 110\,\mu$m of depth for an optical zone of 6 mm with a 0.6 mm transition zone was performed in 20 rabbits. The eye during the femtosecond ablation procedure was immobilized with a suction ring. The ablation time, required for removal of the corneal epithelium, was evaluated by observing the change of intensity of the fluorescence in the blue spectral region [47]. According to published data, we presumed that the thickness of rabbit epithelium is between $32.2\,\mu$m and $47.7\,\mu$m [29, 48–52]. Therefore, we have estimated that during the TransPRK with a central ablation depth of $\sim 110\,\mu$m, the thickness of the removed stromal layer was between $60\,\mu$m and $80\,\mu$m. For the myopic ablation the central thickness of $70\,\mu$m within 6 mm optical zone corresponds to $\sim 5.0\,$D refraction change.

We attempted to perform the same TransPRK ablation using the excimer laser system "Technolas 217z100" ("Technolas Perfect Vision", USA) in 10 rabbits. The epithelium was removed in a 6.6 mm zone using the phototherapeutic keratectomy (PTK) mode, followed by myopic stroma ablation of $70\,\mu$m depth in optical zone of 6 mm. According to the decreased intensity of blue fluorescence (which we assumed to be an indication of complete epithelial removal), the PTK depth was set to $55\,\mu$m. According to the manufacturer's protocol, the procedure was frequently paused.

As the excimer ablation depth unexpectedly resulted in a value of (151.4±

[1]Approval for this study was obtained from the Lithuanian State Food and Veterinary Service (number 0213, issued 2011-02-12)

19.7) μm instead of $\sim$ 110 μm, we have modified femtosecond TransPRK procedure to simulate the excimer ablation. We set central ablation depth to 150 μm and inserted interruptions into the ablation protocol to reproduce the duration of the excimer ablation. Five rabbits, previously treated by the excimer ablation, underwent the modified TransPRK with femtosecond UV pulses for previously untreated eyes.

Corneal ablation speed of femtosecond 205 nm pulses was evaluated from the central corneal thickness measurements, made before ablation and after reepithelialization of the rabbit cornea. It was estimated that for the non-stop procedure the ablation rate was $\sim$ 1.45 s/D, and for the modified TranPRK procedure $\sim$ 1.62 s/D. In the latter case, the speed was calculated by taking into account only the actual ablation time, i. e., with pauses excluded.

An infrared thermal camera (ThermaCAM S65, FLIR Systems, Inc.) was used for the monitoring of the surface heating during ablation procedures. During the non-stop femtosecond TransPRK, the increase in the maximum corneal surface temperature peaked at the end of the procedure and was less than 7 °C (Fig. 4.2, green line). The temporal dependence of the surface temperature was directly related to the laser beam scanning algorithm. Ablation of the epithelium was performed within the area of 6.6 mm in diameter and lasted $\sim$ 15 s. After that, the ablation zone was reduced to 6 mm, and myopic ablation started. During the myopic ablation, the average power density was higher in the center of the ablation zone in contrast to the epithelial ablation, where the laser power was distributed uniformly over the ablated area. The red line in Fig. 4.2 represents the dynamics of the corneal surface temperature during the myopic ablation with excimer laser pulses (epithelial ablation is not included). The observed increase in the corneal surface temperature was less than 4.5 °C during the entire excimer ablation procedure. The lowest corneal surface temperature was registered during the modified femtosecond TransPRK. Due to the pauses, the overall increase in temperature did not exceed 2.5 °C, whereas the maximum temperature increase during the epithelial removal was only 1.5 °C (Fig. 4.2, blue line).

To assess the outcomes of the TranPRK procedure we followed up the corneal haze dynamic of the rabbit cornea. Development of the corneal haze after different treatments is presented in Fig. 4.3. Corneal haze score data was analyzed using the statistical nonparametric Mann–Whitney test ($p = 0.05$). No statistically significant differences were found in the data of the corneal haze score after the non-stop TransPRK with femtosecond

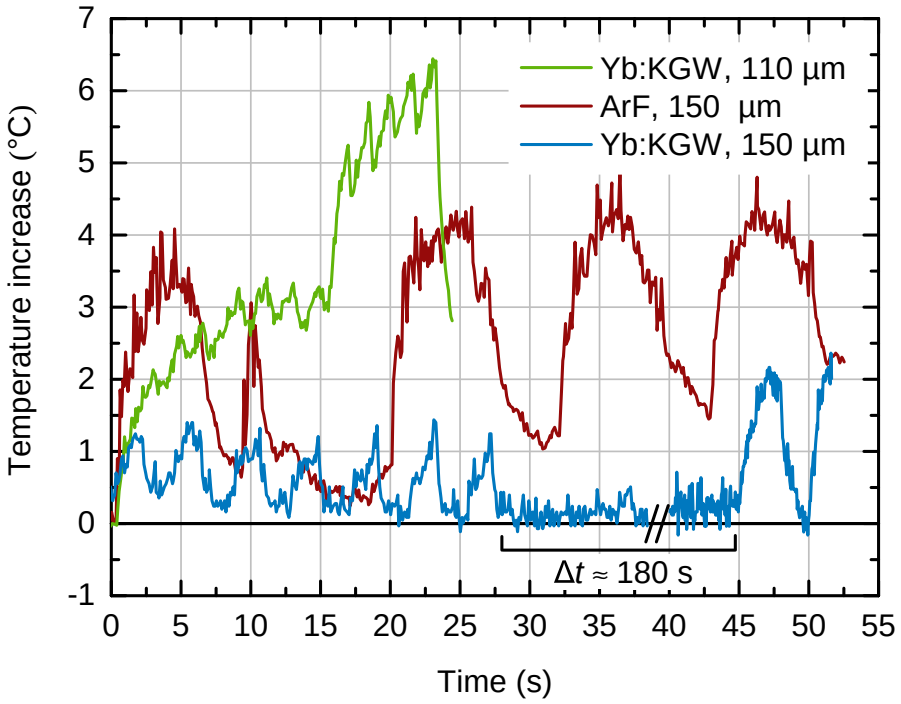

Figure 4.2: Corneal surface temperature changes during the ablation process. Pause between the epithelial and stromal ablations during the modified TransPRK procedure (blue line) is indicated as Δt.

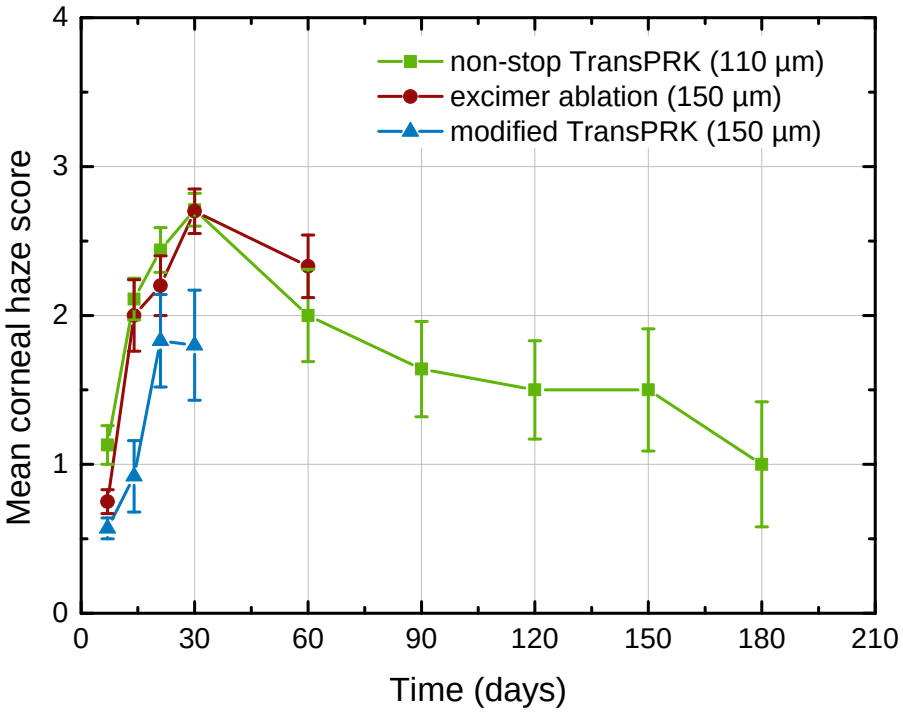

Figure 4.3: Mean corneal central subepithelial haze score dynamics after different treatments.

UV pulses and the excimer laser ablation during the follow-up period of 1 month. The least intense haze was observed after the modified TransPRK treatment. The mean corneal haze score was even lower than after the shallower non-stop TransPRK ablation with femtosecond UV pulses. After evaluation of the amount of haze in the contralateral eyes of the same animals after the excimer ablation and the modified TransPRK, we found that the latter treatment induced less haze. Statistical analysis showed a significant difference in the corneal haze at 1 week and at 1 month after the modified TransPRK with femtosecond UV pulses compared with the haze after the other procedures.

In conclusion, ablation rate of $\sim 1.6\,\mathrm{s}$ per myopic diopter in the 6 mm optical zone was achieved in our experiments without significant impact on the healing outcomes in rabbits. The feasibility of TransPRK is an additional advantage of ablation with femtosecond UV pulses.

Chapter 5

Cytotoxicity and genotoxicity of UV radiation

It is known, that nanosecond pulses of 193 nm and 213 nm wavelenghts induce relatively low levels of the DNA damage and do not cause significant mutagenic tissue changes [31]. In contrast, the wavelengths between 240 nm and 270 nm cause significant DNA damage, because the absorption peak of DNA [31–33]. The wavelength of the fifth-harmonic (205 nm) of the Yb:KGW laser is between 193 nm and 213 nm; however, the impact of the ultrashort high-intensity UV laser pulses on DNA is unknown. In this thesis, we investigated the possible cytotoxic and genotoxic effects of the femtosecond UV pulses on the mice bone marrow and skin epithelial cells *in vitro* and compared it with the impact of the other sources of the UV irradiation. The skin epithelial cells are similar to the corneal epithelial cells.

Male BALB/C mice of 10–12 weeks age and weighing 20–25 g were used. The animals were supplied by the Animal Facility Institute of Immunology, Vilnius University. Ethical approval was given by the Committee of Lithuanian Animal Care and Use.

Four different UV sources we used for irradiation of the bone marrow cell suspension:

- femtosecond pulses of 205 nm, obtained by generating the fifth-harmonic of the solid-state Yb:KGW laser radiation;
- nanosecond pulses of 266 nm and
- nanosecond pulses of 213 nm, obtained using Nd:YAG laser "NL301" ("Ekspla", Lithuania) equipped with the fourth- and fifth-harmonic generation modules;
- 254 nm continuous wave (CW) irradiation (for positive control), ob-

Table 5.1: Parameters of the UV light sources used on bone marrow cells.

	205 nm	213 nm	266 nm	254 nm
Pulse duration	$\sim 500\,\mathrm{fs}$	6 ns	6 ns	-
Pulse repetition rate	20 kHz	10 Hz	10 Hz	-
Energy density (per pulse)	$35\,\frac{\mu\mathrm{J}}{\mathrm{cm}^2}$	$35\,\frac{\mu\mathrm{J}}{\mathrm{cm}^2}$	$35\,\frac{\mu\mathrm{J}}{\mathrm{cm}^2}$	-
Pulse energy	$1.35\,\mu\mathrm{J}$	$\sim 100\,\mu\mathrm{J}$	$\sim 100\,\mu\mathrm{J}$	-
Beam diameter at $1/\mathrm{e}^2$ intensity level	2.2 mm	$\sim 25\,\mathrm{mm}$	$\sim 25\,\mathrm{mm}$	-
Average irradiation power density	$3.5\,\frac{\mathrm{mW}}{\mathrm{cm}^2}$	$0.35\,\frac{\mathrm{mW}}{\mathrm{cm}^2}$	$0.35\,\frac{\mathrm{mW}}{\mathrm{cm}^2}$	$0.35\,\frac{\mathrm{mW}}{\mathrm{cm}^2}$

tained by using a mercury discharge lamp.

The parameters of the irradiation sources are presented in Table 5.1.

Comet assay (single-cell gel electrophoresis) was used for the DNA damage measurement. The cytotoxicity assessment of irradiation of different UV sources was performed using Trypan blue exclusion as an integral part of the comet assay. One should keep it in mind, that if the viability of cells is less than 25 % (compared to the control level of the non-irradiated cells), results of the comet assay are ambiguous and include not only genotoxic but also cytotoxic effects.

The results of the assessment of cytotoxicity and genotoxicity are presented in Fig. 5.1. It is evident that the irradiation of shorter wavelengths (205 nm and 213 nm) had stronger cytotoxic effect than the the irradiation of longer wavelengths (266 nm and 254 nm). The comet assay revealed, that the genotoxic impact is also more likely related with the wavelength of the radiation rather than with the pulse duration. Nanosecond 213 nm pulses caused similar amount of the DNA damage, compared to the femtosecond 205 nm pulses; the impact of the CW 254 nm radiation was identical with nanosecond 266 nm pulses.

Evaluation of the DNA damage, made by each radiation source, is presented in Table 5.2. Since the viability of the non-irradiated cells was (85.1 ± 0.3) %, the DNA damage, for which the viability did not decrease significantly (i. e. was higher than 80 %), indirectly reflects the probability for a cell to mutate. Our results show, that the femtosecond laser pulses of 205 nm had the lowest impact on DNA of the bone marrow cells compared to the other irradiation sources.

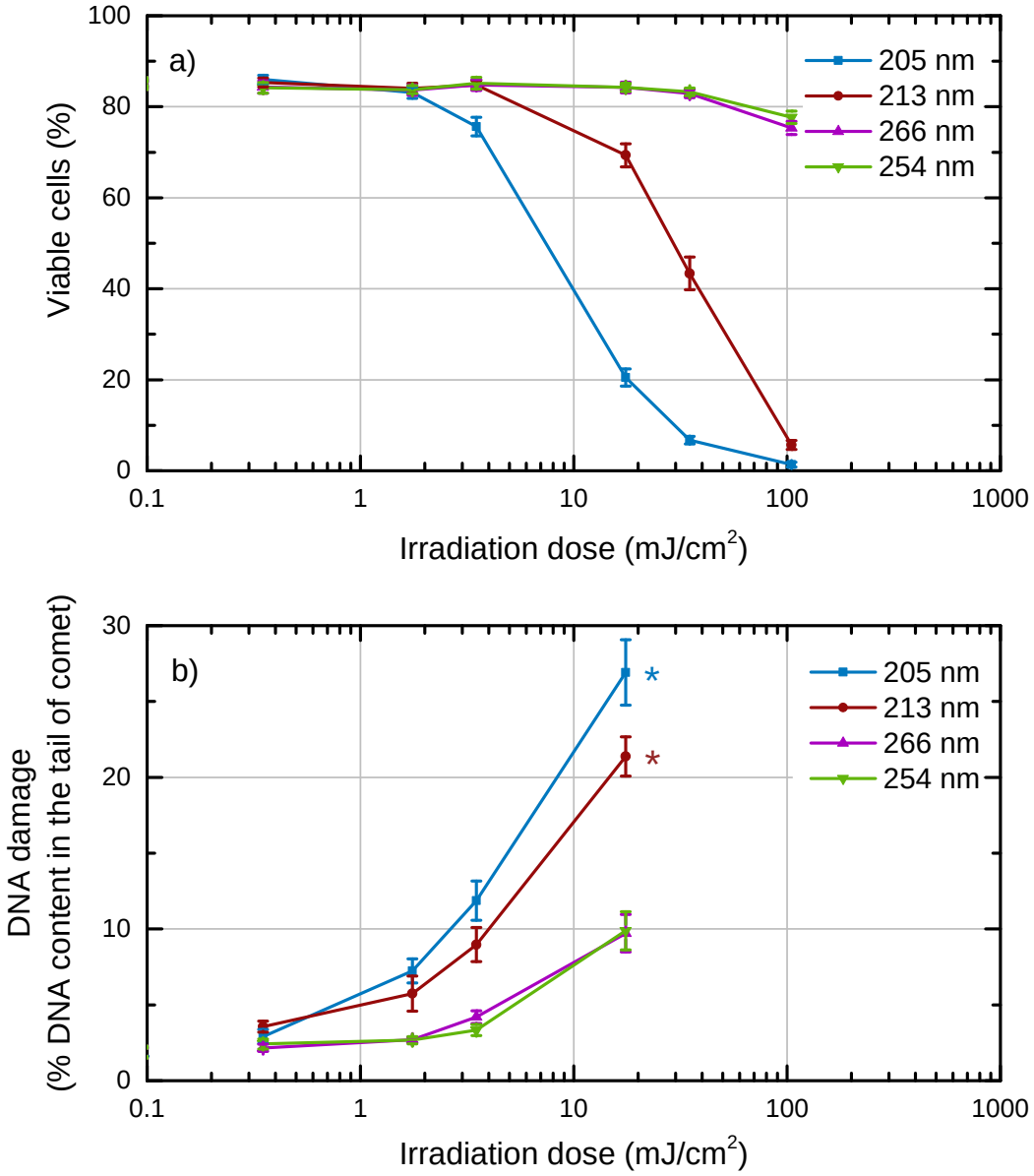

Figure 5.1: Dependence of viability of the bone marrow cells (a) and the DNA damaging effect (b) on the irradiation dose for different UV radiation. Data points, which might have been influenced by the decreased cell viability, are indicated by asterisks (see text for details).

The skin epithelial cells are bigger (mean diameter $35.9 \pm 2.0\,\mu$m) than the bone marrow cells (mean diameter $7.6 \pm 0.2\,\mu$m) and are usually exposed to the natural UV light. We have evaluated the DNA damage of the UV radiation to the mice skin epithelial cell suspension by irradiating it with the fourth- (257 nm) and the fifth-harmonic (205 nm) pulses of the femtosecond Yb:KGW laser and the 254 nm CW radiation of the mercury discharge lamp. The pulse repetition rate of the femtosecond laser was 50 kHz and the average power density for both 257 nm and 205 nm pulses was $1.4\,\mathrm{mW/cm^2}$.

Table 5.2: Wavelength of irradiation source λ, dose, viable cells percentage and the DNA damage value in the cases when the cell viability was higher than 80 %.

λ(nm)	Dose (mJ/cm^2)	Viable cells (%)	DNR damage (% DNA content in the tail of comet)
205	1.75	83.1 ± 1.2	7.24 ± 0.8
213	3.5	84.8 ± 1.0	9.0 ± 1.1
266	17.5	84.3 ± 1.2	9.7 ± 1.2
254	17.5	84.3 ± 0.9	9.9 ± 1.3

The average power density of the 254 nm radiation varied from 0.8 mW/cm^2 to 0.9 mW/cm^2. The exposure time for each UV source was calculated by dividing the dose by the average irradiation power density.

The results of the cytotoxic and genotoxic impact assessment on mice skin epithelial cells are presented in Fig. 5.2. The femtosecond 205 nm pulses had the strongest cytotoxic effect, while the viability of the skin epithelial cells irradiated with the femtosecond 257 nm pulses and 254 nm CW radiation was identical. The lowest damaging effect of DNA was found after irradiation with the femtosecond 205 nm pulses. The highest level of the DNA damage was found in samples, which were exposed with the femtosecond 257 nm radiation.

In the same way as for the bone marrow cells, we evaluated the DNA damage at the same level of cytotoxicity for each particular radiation source by selecting the DNA damage value at the highest dose, that did not reduce the viability of the cells significantly. These values of the DNA damage are presented in Table 5.3. It is evident, that 205 nm femtosecond pulses are less genotoxic than the radiation of 257 nm and 254 nm wavelengths.

Table 5.3: Wavelength of irradiation source λ, dose, viable cells percentage and the DNA damage value in the cases when the cell viability was higher than 70 %.

λ(nm)	Dose (mJ/cm^2)	Viable cells (%)	DNR damage (% DNA content in the tail of comet)
205	1.75	75.2 ± 2.0	4.6 ± 0.4
257	17.5	74.0 ± 1.8	30.1 ± 2.8
254	17.5	73.6 ± 2.6	18.6 ± 2.4

In vitro experiments with the mice bone marrow and the skin epithelial

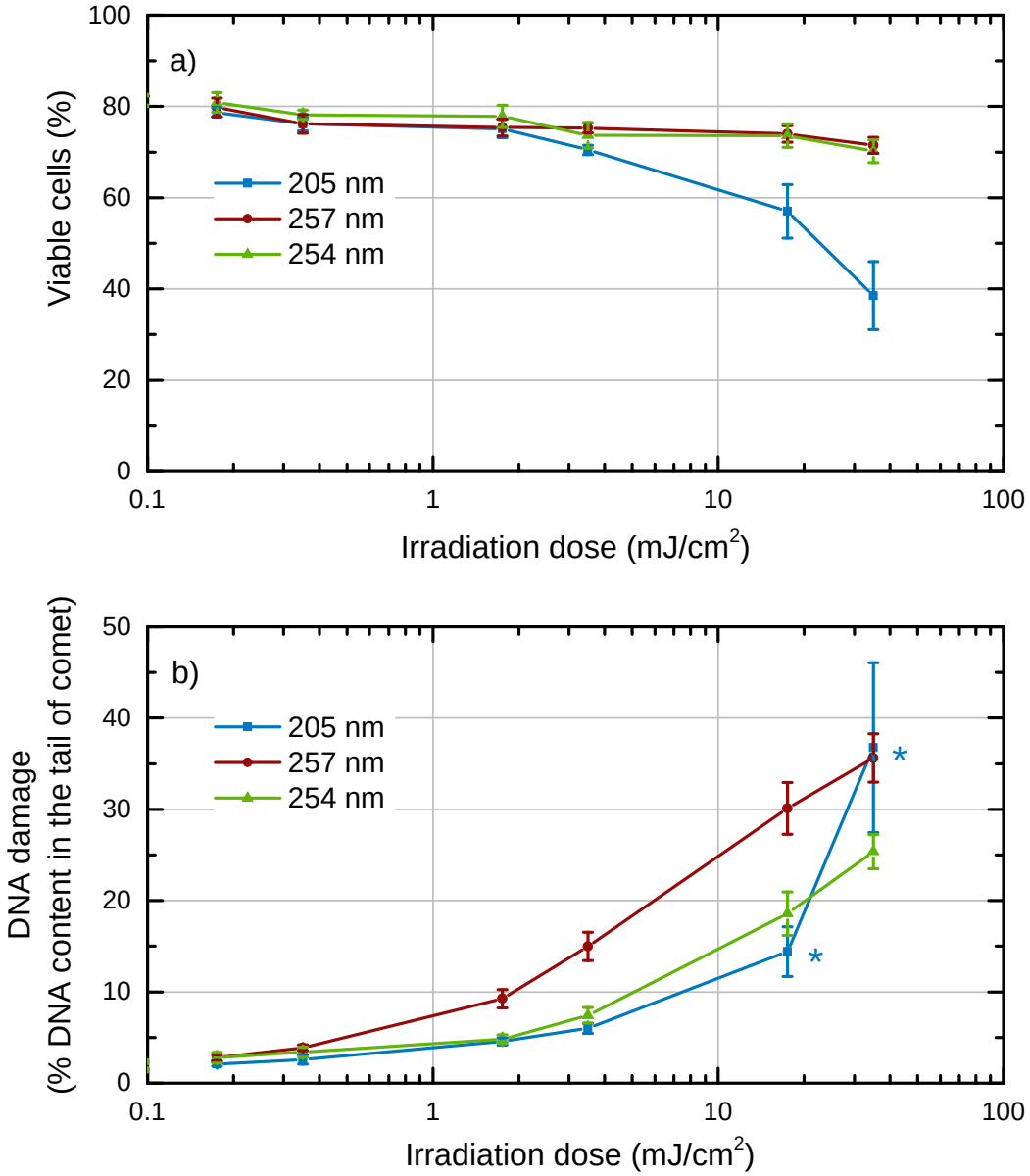

Figure 5.2: Dependence of viability of the skin epithelial cells (a) and the DNA damaging effect (b) on the irradiation dose for different UV irradiation sources. Data points, which might have been influenced by decreased cell viability, are indicated by asterisks (see text for details).

cells revealed, that femtosecond 205 nm and nanosecond 213 nm UV pulses have significantly higher impact on viability of cells than the radiation of longer wavelengths (254 nm, 266 nm or 257 nm). The amount of DNA damage at the shorter wavelengths strongly depends on the size of the cell because of the penetration depth of the UV radiation. If the wavelength of UV radiation is shorter than 220 nm, the radiation is strongly absorbed by the outer layers of the cell [33]. Therefore, the smaller cells, like mice bone marrow cells, are more sensitive to the shorter UV radiation, because

the penetration depth could be enough to reach the nucleus of the cell. If the cell is large enough, like the mice skin epithelial cell, the entire amount of short UV radiation is absorbed in the superficial layer, and the DNA within the nucleus of the cell remains unaffected. That is why the short UV wavelengths have strong cytotoxic (they easily harm the membrane of the cell) and quite weak genotoxic impact (the nucleus is firmly shielded by the outer layers). In contrast, the absorption of the longer UV wavelengths (240–270 nm) is quite low in membrane and cytoplasm of the cell, but is very high in DNA [33]. Therefore, longer UV wavelengths only slightly harm the outer layers of the cell, but induce substantially higher genotoxic effect by damaging DNA. Because of the large penetration depth of 240–270 nm radiation, the genotoxic impact remains almost the same for the cells of different sizes.

We have demonstrated, that the impact of the UV radiation is more related with the wavelength of light than with the pulse duration. The probability of the mutagenic impact of the femtosecond 205 nm pulses is very low because of the low genotoxicity and the high cytotocixity, which in turn reduce the possibility for the cells with damaged DNA to survive.

Chapter 6

Femtosecond nIR pulses in refractive corneal surgery

Corneal flap is usually created using the nIR femtosecond pulses. There are two different techniques to control the tightly focused laser beam inside the cornea. First one is to scan laser beam with the galvanometric mirror scanners through the large-aperture f–theta lens. All contemporary commercial laser systems for refractive eye surgery, except one ("Femto LDV", "Ziemer Ophthalmic Systems", Switzerland), are based on this method. The main disadvantage of this method is the expensive and complicated focusing objective with limited numerical aperture NA (typically $NA \leq 0.3$ [53]). The second technique is to scan a small lens of high NA in x, y an z directions together with the supporting mirrors, while maintaining the direction and the position of the beam fixed with respect to the focusing lens [54]. Using the femtosecond Yb:KGW laser as the radiation source we have tested both techniques for creation of the corneal LASIK flap.

In the first part of the corneal flap cutting experiments, we used galvanometric mirror scanners and the customized f–theta lens. The cornea was immobilized using a curved applanation interface with a suction ring (Fig. 6.1, a). The femtosecond laser beam was focused using a lens L_2 ($f = +500\,\mathrm{mm}$) to an pinhole PH of $125\,\mu\mathrm{m}$ in diameter, which transmitted about 85 % of radiation and acted as a spatial filter improving the beam quality. Position of the lens L_3 was controlled using a motorized positioning stage MPS to change the beam focusing depth inside the cornea. Nearly collimated beam (behind L_4) was scanned before the focusing objective ($f = +50\,\mathrm{mm}$, $NA \approx 0.1$) using a pair of galvanometric scanners ("intelliSCAN® 10", "Scanlab", Germany). The estimated beam waist inside the cornea was $\sim 4.5\,\mu\mathrm{m}$ (radius at the $1/\mathrm{e}^2$ intensity level). Before

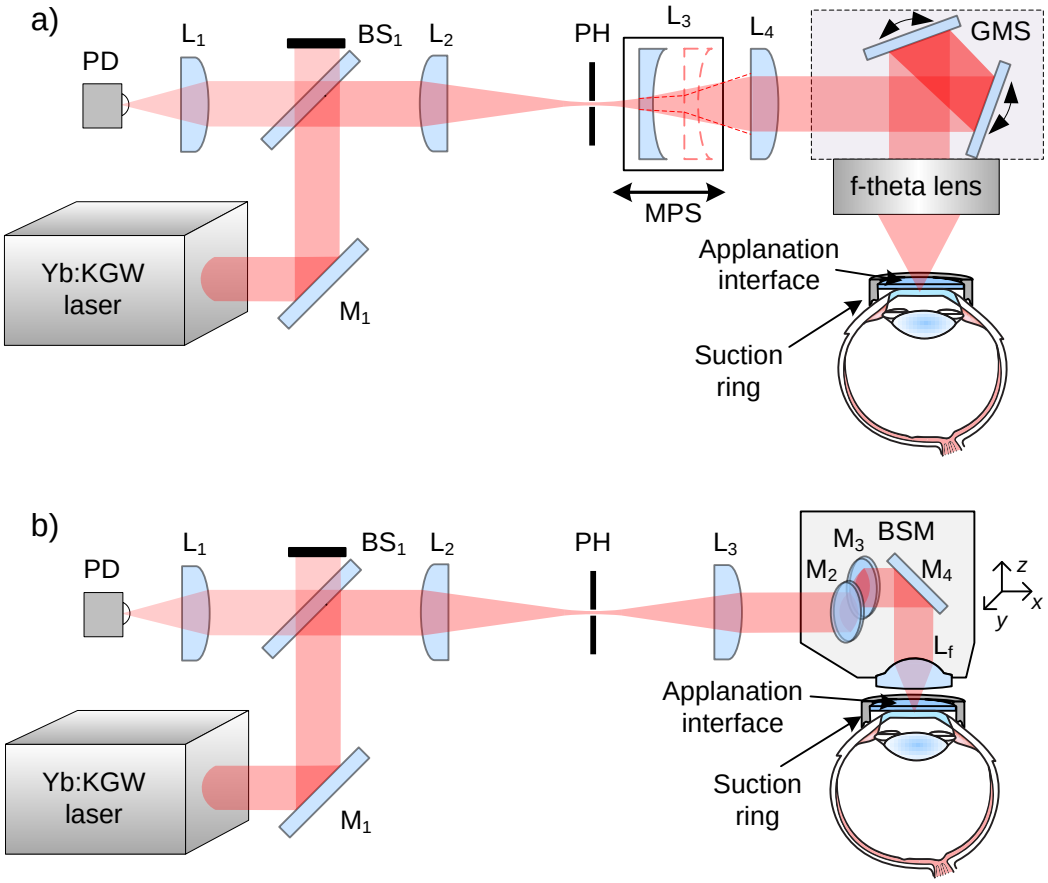

Figure 6.1: Experimental setups for the corneal flap creation: a) with a f–theta focusing lens and b) with a focusing lens of high *NA*. L_1–L_4 – lenses, M_1–M_4 – mirrors, BS_1 – beam splitter, MPS – motorized positioning stage, GMS – galvanometer mirror scanner, PD – photodiode, PH – pinhole, BMS – beam scanning module, L_f – focusing lens.

the corneal flap creation procedure, the position of the beam waist with respect to the applanation interface was calibrated using confocal method by shifting the lens L_3 in the direction of the beam propagation. The radiation is reflected from the surfaces near the objective focal point, returns through the focusing optics, passes the aperture A and the beamsplitter BS_1 to be registered by the photodiode PD. The intensity dependence of the reflected radiation on the position of the focus exhibits two sharp peaks corresponding to the two surfaces of the applanation glass. Using the positions of these two peaks as a reference, the intended flap thickness was controlled accurately.

The corneal flap was created in *ex vivo* porcine eye by scanning the focused laser beam in a spiral pattern. The pulse repetition rate was 200 kHz, the axial and radial distances between adjacent spots were 3 μm and 8 μm, respectively. The time required for forming a corneal flap of 10 mm diam-

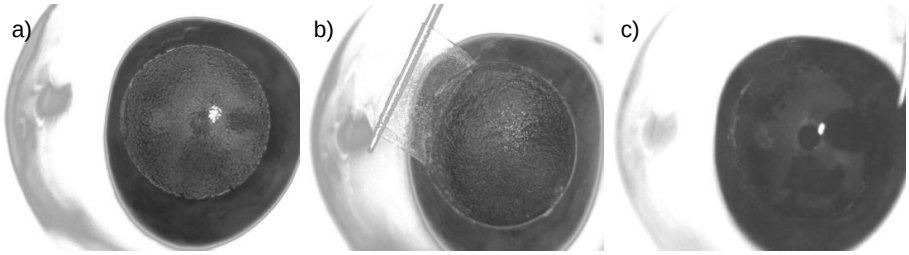

Figure 6.2: Corneal flap, created using f–theta lens, before the opening (a), corneal surface view with the flap lifted (b) and after replacing the flap (c).

eter with pulse energy of about 1 μJ was 20 s. The 80° side-cut was made with the same pulse energy as the bed cut, with spot separation distance of 3 μm.

Corneal flap was easily lifted using a surgical spatula and the measured thickness of the flap was $\sim$ 100 μm. However, the corneal surface after opening the flap was quite rough (Fig. 6.3). It was also noted, that using f–theta focusing objective of low *NA* the thickness of the flap depends on the average radiation power. When the critical self-focusing power value is exceeded, the thickness of corneal flap decreases [55].

The second method to create the bubble layer inside the cornea is to scan the laser beam together with a focusing lens of high *NA*. The optical setup for the corneal flap creation is presented in Fig. 6.1, b. The pulse repetition rate of the laser system was 1 MHz and the pulse duration was $\sim$ 325 fs.

Ex vivo corneal flap was created using the focusing lens of $NA \approx 0.3$. The distance between the adjacent laser pulses was set to 3 μm while the energy of the pulse was 160 nJ. Corneal flap of 9 mm in diameter was created in 12 s. We have demonstrated, that the flaps of different thickness from 30 μm to 250 μm can be created and easily lifted without any ripping (Fig. 6.3). The corneal surface appeared smoother after lifting the flap, which was created using the high *NA* lens (Fig. 6.3, d), than one created with the low *NA* f–theta objective (Fig. 6.2, b). After replacing the flap the surface of the cornea remained clear and smooth (Fig. 6.3, h). We have created 12 corneal flaps in *ex vivo* porcine corneas with the same intended thickness of 110 μm and measured the thickness of the separated flaps. We found that the mean thickness 109.2 ± 12.4 μm was very close to the intended value.

To estimate the capabilities of our prototype laser system, we performed an all-femtosecond myopic correction in *ex vivo* porcine eye. Using the focusing lens of the high *NA* we cut a lens like structure inside the corneal stroma and removed it through the small incision (Fig. 6.4). This procedure is called SmILE (Small Incision Lenticule Extraction) and currently

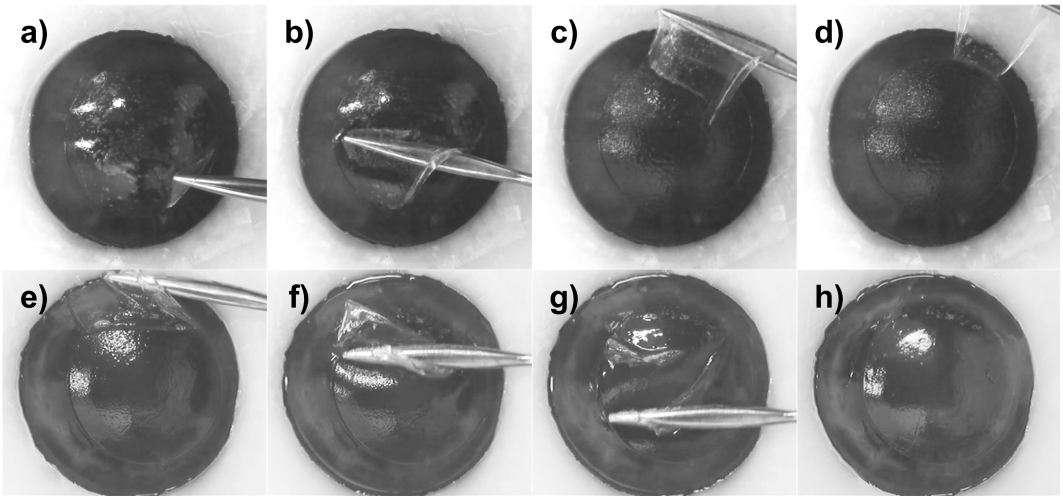

Figure 6.3: With the lens of high *NA* created corneal flap was easily lifted (a–d) and replaced (e–h).

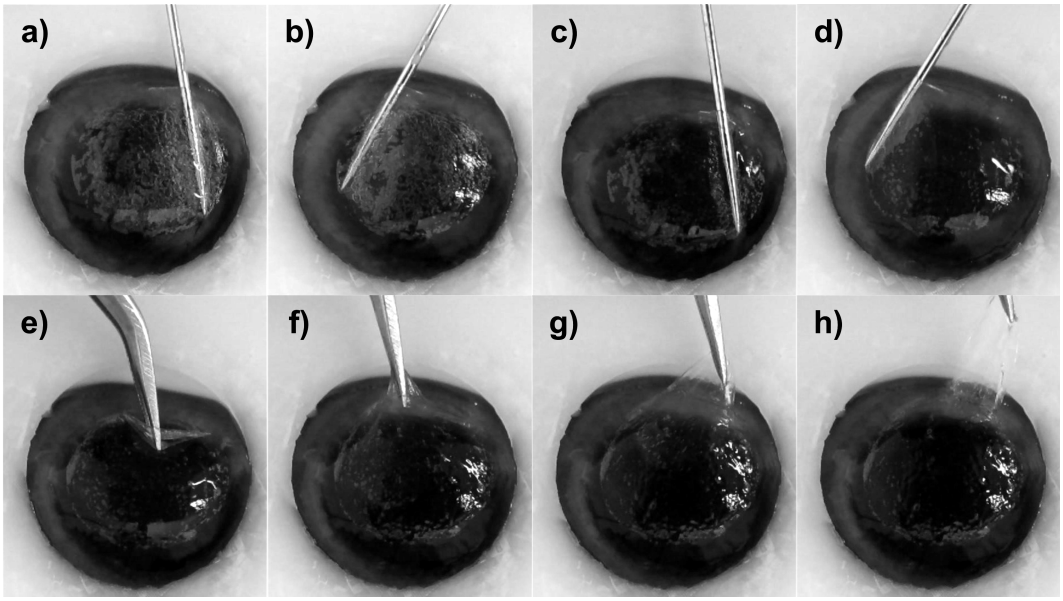

Figure 6.4: Extraction of the corneal lenticule through the small incision. Separation of the bottom (a and b) and the top (c and d) surfaces of the corneal lenticule. Removal of the separated corneal layer through the small side cut (e–h).

there is only one commercial femtosecond system ("Visumax", "Carl Zeiss Meditec", Germany), which is capable to perform it. The corneal lenticule was easily separated using a spatula and was removed using forcepts in one piece through the small incision (Fig. 6.4).

The procedure of the LASIK flap creation, using modern commercial femtosecond laser systems, lasts from 8 s to 60 s [56, 57]. We have demonstrated that the corneal flap can be created in 12 s. The quality of the intrastromal cut allows us to create the corneal flaps as thin as 30 μm and

to perform all-femtosecond correction of refractive errors.

When the Yb:KGW femtosecond laser is equipped with the fifth-harmonic generator, it becomes a universal and powerful surgical tool for variety of ophthalmic surgeries. It is capable to perform:

- the full LASIK procedure by creating the corneal flap with nIR pulses and subsequently reshaping the curvature of the corneal surface using the fifth-harmonic UV pulses;
- SmILE procedure – the all-femtosecond correction of the refractive errors;
- various intrastromal cuts with nIR pulses (treatment of presbyopia, corneal transplantation or pockets for intrastromal implants);
- transepithelial ablations of the cornea;
- retreatment after all-femtosecond refractive correction procedure.

Santrauka

Refrakcinės regos ydos – trumparegystė, toliaregystė, presbiopija ir astigmatizmas – daro didelę įtaką žmogaus gyvenimo kokybei. Pastaraisiais dešimtmečiais visame pasaulyje trumparegystė diagnozuojama vis dažniau ir vis jaunesniems [1–7]. Pavyzdžiui, kai kuriuose Azijos regionuose šiandien daugiau kaip 90 % paauglių yra trumparegiai [1, 8]. Ne išimtis ir Lietuva – remiantis 2013 m. Lietuvos Sveikatos apsaugos ministerijos duomenimis per ketverius metus nuo 2010 m. gydymo įstaigose užregistruotų trumparegystės atvejų padaugėjo nuo 57,6 iki 63,5, o toliaregystės – nuo 58,5 iki 96,7 tūkstančiui gyventojų. Nors daugeliu atvejų refrakcinės ydos netgi nėra traktuojamos kaip liga (nes gali būti visiškai koreguojamos akiniais arba kontaktiniais lęšiais), didelės refrakcinės ydos gali sukelti kitas akių ligas: kataraktą, glaukomą, tinklainės ligas ir netgi aklumą [58].

Lazerinė refrakcinė chirurgija – tai alternatyva akiniams ir kontaktiniams lęšiams, kuri leidžia pagerinti paciento gyvenimo kokybę. Šiandien viena iš dažniausiai atliekamų lazerinės refrakcinės chirurgijos procedūrų yra lazerinė *in situ* keratomilezė (LASIK) [9]. Šios procedūros metu chirurginiu skalpeliu arba femtosekundine artimosios infraraudonosios srities (aIR) lazerine spinduliuote (tada procedūra vadinama Femto-LASIK [10]) atpjaunamas plonas viršutinis ragenos sluoksnis (lopas), o jį atvertus gilesniuose stromos audiniuose ultravioletiniais (UV) nanosekundiniais impulsais formuojamas refrakcijos pokytis. Po procedūros atgal užklotas ragenos lopas grąžina ragenos paviršiaus optinę kokybę.

Pirmą kartą femtosekundiniais impulsais ragenos lopas žmogaus akyje buvo atpjautas gana neseniai, 2001 m. [59]. Nuo to laiko femtosekundiniai lazeriai įsitvirtino oftalmologijoje dėl itin tikslių ir taisyklingos geometrijos intrastrominių pjūvių [60], didesnio saugumo [11–14], greitesnio pooperacinio gijimo ir geriau prognozuojamų refrakcinės chirurgijos baigčių [15, 16]. Didžiausias Femto-LASIK procedūros trūkumas yra tai, kad vienai procedūrai atlikti reikia dviejų lazerinių sistemų, kurios generuoja femtosekundinius aIR ir nanosekundinius UV impulsus. Dėl to gydytojas turi išmokti valdy-

ti abi sistemas (dažniausiai skirtingų gamintojų), kiekvieną kartą atskirai abiems lazeriams nustatyti procedūros parametrus; taip pat operacijos metu tenka perkelti pacientą nuo vienos sistemos prie kitos. Visa tai ilgina bendrą Femto-LASIK procedūros trukmę ir kelia nepatogumų tiek gydytojui, tiek pacientui. Negana to, abi lazerinės sistemos yra brangios bei užima nemažai vietos.

Situacija smarkiai pasikeistų, jeigu visa LASIK procedūra būtų atliekama naudojant vieną lazerinę sistemą. Per pastarąjį dešimtmetį smarkiai patobulėjus kietakūnių femtosekundinių lazerių technologijoms, atsirado techninė galimybė turėti vieno Yb:KGW lazerio pagrindu veikiantį šviesos šaltinį, generuojantį ir UV, ir aIR srities femtosekundinius impulsus. Mūsų tikslas – ištirti, ar tokio lazerinio šaltinio pagrindu sukurta refrakcinės regos korekcijos sistema galėtų pakeisti ir aIR, ir UV srities lazerius, šiuo metu naudojamus refrakcinei chirurgijai.

Siekiant šio tikslo buvo suformuluoti pagrindiniai uždaviniai:

1. Surinkti ir optimizuoti femtosekundinio Yb:KGW lazerio penktosios harmonikos (205 nm) generatorių ir, optimizavus lazerinės sistemos parametrus, įvertinti *ex vivo* ir *in vivo* ragenos stromos abliacijos spartą.

2. Optimizuoti abliacijos algoritmą išlaikant minimalų šiluminį poveikį ragenos audiniams, aukštą paviršiaus kokybę bei didelę trumparegystės korekcijos spartą.

3. Įvertinti femtosekundiniais UV impulsais operuotų *in vivo* triušio ragenų paviršiaus kokybę, gijimo tendencijas ir patologinius pakitimus bei palyginti šiuos rezultatus su gautaisiais naudojant komercinę nanosekundinę argono fluorido (ArF) lazerinę sistemą.

4. Pritaikyti Yb:KGW lazerinės sistemos aIR srities impulsus LASIK ragenos lopo pjovimui ir laužiamąją ragenos gebą keičiančių tūrinių darinių formavimui. Ištirti, kaip suformuotų darinių optinė kokybė, tikslumas ir atkartojamumas priklauso nuo pluošto fokusavimo sistemos bei lazerinės spinduliuotės parametrų.

5. Įvertinti femtosekundinės ultravioletinės spinduliuotės citotoksinį[1] ir genotoksinį[2] poveikį gyvoms ląstelėms bei palyginti jį su kitų ultravioletinės spinduliuotės šalinių poveikiu.

[1]Citotoksinis – ([gr.] kytos – ląstelė + [gr.] toxikon – nuodai) žudantis ląstelę

[2]Genotoksinis – pažeidžiantis ląstelės DNR

Ginamieji teiginiai

1. Dideliu pasikartojimo dažniu veikiančių ketvirtosios ir aukštesniųjų harmonikų femtosekundinių impulsų generatorių spinduliuotės moduliavimo spartą riboja UV spinduliuotės sugertis netiesiniuose kristaluose. Moduliavimo spartą galima padidinti tūkstančius kartų adaptyviai valdant netiesinio optinio kristalo fazinio sinchronizmo derinimo kampą.

2. Femtosekundiniais Yb:KGW kietakūnio lazerio fundamentinės aIR spinduliuotės impulsais ragenos lopas suformuojamas tiksliai ir atkartojamai; ši lazerinė sistema lopo formavimo procedūros trukme nenusileidžia šiuolaikinėms komercinėms sistemoms.

3. Femtosekundinė Yb:KGW lazerinė sistema ragenos stromos abliacijos sparta ir kokybe prilygsta komercinėms eksimerinėms ArF lazerinėms sistemoms.

4. Citotoksinis ir genotoksinis UV spinduliuotės poveikis ląstelei stipriai priklauso nuo bangos ilgio ir beveik nepriklauso nuo impulso trukmės. Esant vienodoms apšvitos dozėms, femtosekundinių 205 nm bangos ilgio impulsų genotoksinis poveikis neviršija oftalmologinėms procedūroms naudojamų nanosekundinių UV impulsų genotoksinio poveikio.

5. Dauguma lazeriu atliekamų šiuolaikinių refrakcinių akies ydų korekcijos procedūrų, gali būti atliktos naudojant vieną femtosekundinę Yb:KGW kietakūnę lazerinę sistemą su penktosios harmonikos generatoriumi.

Mokslinio darbo naujumas ir reikšmė

Yra žinoma, kad šiluminiai reiškiniai UV harmonikų generatoriuose mažina generavimo efektyvumą, blogina pluošto charakteristikas bei keičia fazinio sinchronizmo sąlygas [21, 61]. Kai konvertuojami ilgi nanosekundiniai ar pikosekundiniai impulsai, šiluminių reiškinių įtaka mažinama naudojant įvairius kristalo aušinimo metodus [22–24]. Tačiau generuojant didelio pasikartojimo dažnio (dešimčių kilohercų ir daugiau) ultratrumpuosius UV impulsus, paprastai naudojami itin ploni (iki 1 mm storio) netiesiniai optiniai kristalai, kuriems praktiškai pritaikyti standartinius aušinimo metodus beveik neįmanoma. Šiame darbe pirmą kartą išsamiai charakterizuoti pereinamieji reiškiniai kelių dešimčių kilohercų pasikartojimo dažniu veikiančio femtosekundinio lazerio UV harmonikų generatoriuje. Pasiūlyti nauji šiluminių reiškinių įtakos sumažinimo būdai, kurie galėtų būti pritaikomi la-

zeriniam medžiagų apdirbimui. Tai leistų sumažinti vidutinės spinduliuotės galios svyravimus laike bei pagreitinti lazerinio apdirbimo procesus.

Kietojo kūno nanosekundiniai lazeriai su UV harmonikų generatoriais refrakcinėje akių chirurgijoje taikomi nuo 2004 m. [25, 26]. Ir nors ragenos stromos abliacijos rezultatai visiškai tenkina refrakcinei chirurgijai keliamus reikalavimus [27–29], šioms sistemoms nėra lengva konkuruoti su tradicinėmis eksimerinėmis ArF lazerinėmis sistemomis, kurios toms pačioms refrakcinės regos korekcijos procedūroms pradėtos taikyti kur kas anksčiau [62]. Mūsų žiniomis, šiame darbe pristatoma ragenos stromos abliacija femtosekundinio Yb:KGW kietojo kūno lazerio penktosios harmonikos (205 nm) impulsais buvo atlikta pirmą kartą. Lyginant su nanosekundiniais impulsais, femtosekundiniai impulsai pasižymi tuo, kad dėl trumpesnės sąveikos trukmės abliacijos metu ragenos paviršius mažiau kaista.

Šiuo metu jokia lazerinė sistema, galinti atlikti ir stromos abliaciją, ir ragenos lopo formavimą, nėra komerciškai prieinama. Nors „Katana Technologies“ (Vokietija) jau kuris laikas savo elektroninėje svetainėje skelbia apie tokį produktą [30], jokių su šia sistema susijusių publikacijų rasti nepavyko. Mūsų darbe pademonstruota galimybė viena femtosekundine lazerine sistema atlikti pilną Femto-LASIK procedūrą. Sukūrus universalią femtosekundinę lazerinę sistemą palengvėtų chirurgo darbas: LASIK operacija truktų trumpiau, nes nereiktų perkelti paciento ir derinti dviejų lazerinių sistemų, viena integruota valdymo sistema abiems LASIK procedūros etapams sumažintų klaidos tikimybę, ta pačia sistema būtų galima atlikti ir kitas, vien tik femtosekundiniais impulsais atliekamas procedūras: keratoplastikos operacijas, refrakcijos ir presbiopijos korekciją.

Yra žinoma, kad trumpesnio UV bangos ilgio spinduliuotė (193–210 nm) sukelia žymiai mažesnį genotoksinį poveikį ląstelėse nei ilgesnio, $\sim 260\,\mathrm{nm}$ bangos ilgio spinduliuotė [31, 32]. Tačiau iki šiol nebuvo ištirta, kaip keičiasi citotoksinis ir genotoksinis spinduliuotės poveikis trumpėjant impulso trukmei, kai šviesos intensyvumas skiriasi tūkstančius kartų. Mes įvertinome femtosekundinės UV spinduliuotės citotoksinį ir genotoksinį poveikį pelių kaulų čiulpų ir odos epitelio ląstelėms bei palyginome gautus rezultatus su kitų UV spinduliuotės šaltinių poveikiais. Lyginant su nanosekundiniais 213 nm impulsais, didesnis femtosekundinių 205 nm impulsų citotoksinis poveikis ląstelėms esant panašiam genotoksiniam poveikiui gali būti laikomas privalumu, nes mažėja tikimybė, kad mutavusi ląstelė (su pažeista ir netinkamai atkurta DNR) sugebės replikuotis.

Bibliography

[1] E. Dolgin, The myopia boom, Nature **519**(7543), 276–278 (2015).

[2] I. G. Morgan, K. Ohno-Matsui, S.-M. Saw, Myopia, Lancet **379**(9827), 1739–1748 (2012).

[3] S. Vitale, R. D. Sperduto, F. L. Ferris, Increased prevalence of myopia in the United States between 1971-1972 and 1999-2004, Arch. Ophthalmol. **127**(12), 1632–1639 (2009).

[4] S. Jobke, E. Kasten, C. Vorwerk, The prevalence rates of refractive errors among children, adolescents, and adults in Germany, Clin. Ophthalmol. **2**(3), 601 (2008).

[5] S.-M. Saw, Y.-H. Chan, W.-L. Wong, A. Shankar, M. Sandar, T. Aung, D. T. Tan, P. Mitchell, T. Y. Wong, Prevalence and risk factors for refractive errors in the Singapore Malay Eye Survey, Ophthalmology **115**(10), 1713–1719 (2008).

[6] M. G. Villarreal, J. Ohlsson, M. Abrahamsson, A. Sjöström, J. Sjöstrand, Myopisation: The refractive tendency in teenagers. Prevalence of myopia among young teenagers in Sweden, Acta Ophthalmol. Scand. **78**(2), 177–181 (2000).

[7] C.-W. Pan, D. Ramamurthy, S.-M. Saw, Worldwide prevalence and risk factors for myopia, Ophthalmic Physiol. Opt. **32**(1), 3–16 (2012).

[8] J. F. Wu, H. S. Bi, S. M. Wang, Y. Y. Hu, H. Wu, W. Sun, T. L. Lu, X. R. Wang, J. B. Jonas, Refractive error, visual acuity and causes of vision loss in children in Shandong, China. The Shandong children eye study, PLoS ONE **8**(12), e82763 (2013).

[9] D. Z. Reinstein, T. J. Archer, M. Gobbe, The history of LASIK, J. Refract. Surg. **28**(4), 291–298 (2012).

[10] M. Ghoreishi, A. Naderi Beni, Z. Naderi Beni, Visual outcomes of Femto-LASIK for correction of residual refractive error after corneal

graft, Graefes Arch. Clin. Exp. Ophthalmol. **251**(11), 2601–2608 (2013).

[11] I. Ratkay-Traub, I. E. Ferincz, T. Juhasz, R. M. Kurtz, R. R. Krueger, First clinical results with the femtosecond neodynium–glass laser in refractive surgery, J. Refract. Surg. **19**(2), 94–103 (2002).

[12] K. Stonecipher, T. S. Ignacio, M. Stonecipher, Advances in refractive surgery: microkeratome and femtosecond laser flap creation in relation to safety, efficacy, predictability, and biomechanical stability, Curr. Opin. Ophthalmol. **17**(4), 368–372 (2006).

[13] A. A. Farjo, A. Sugar, S. C. Schallhorn, P. A. Majmudar, D. J. Tanzer, W. B. Trattler, J. B. Cason, K. E. Donaldson, G. D. Kymionis, Femtosecond lasers for LASIK flap creation: A report by the American Academy of Ophthalmology, Ophthalmology **120**(3), e5–e20 (2013).

[14] J. A. Davison, S. C. Johnson, Intraoperative complications of LASIK flaps using the intralase femtosecond laser in 3009 cases, J. Refract. Surg. **26**(11), 851 (2010).

[15] M. Tanna, S. C. Schallhorn, K. A. Hettinger, Femtosecond laser versus mechanical microkeratome: A retrospective comparison of visual outcomes at 3 months, J. Refract. Surg. **25**(7), S668–S671 (2009).

[16] D. S. Durrie, G. M. Kezirian, Femtosecond laser versus mechanical keratome flaps in wavefront-guided laser *in situ* keratomileusis: Prospective contralateral eye study, J. Cataract Refract. Surg. **31**(1), 120–126 (2005).

[17] W. Sekundo, K. S. Kunert, M. Blum, Small incision corneal refractive surgery using the small incision lenticule extraction (SMILE) procedure for the correction of myopia and myopic astigmatism: Results of a 6 month prospective study, Br. J. Ophthalmol. **95**(3), 335–339 (2011).

[18] M. Blum, K. S. Kunert, U. Voßmerbäumer, W. Sekundo, Femtosecond lenticule extraction (ReLEx®) for correction of hyperopia – first results, Graefes Arch. Clin. Exp. Ophthalmol. **251**(1), 349–355 (2013).

[19] A. K. Riau, R. I. Angunawela, S. S. Chaurasia, D. T. Tan, J. S. Mehta, Effect of different femtosecond laser-firing patterns on collagen disruption during refractive lenticule extraction, J. Cataract Refract. Surg. **38**(8), 1467–1475 (2012).

[20] S. Wu, G. A. Blake, S. Sun, H. Yu, Two-photon absorption inside β-BBO crystal during UV nonlinear optical conversion, Proc. SPIE **3928**, 221–227 (2000).

[21] A. Dubietis, G. Tamošauskas, A. Varanavičius, G. Valiulis, Two-photon absorbing properties of ultraviolet phase-matchable crystals at 264 and 211 nm, Appl. Optics **39**(15), 2437–2440 (2000).

[22] C. Rothhardt, J. Rothhardt, A. Klenke, T. Peschel, R. Eberhardt, J. Limpert, A. Tünnermann, BBO-sapphire sandwich structure for frequency conversion of high power lasers, Opt. Mater. Express **4**(5), 1092–1103 (2014).

[23] Y. Yap, K. Deki, N. Kitatochi, Y. Mori, T. Sasaki, Alleviation of thermally induced phase mismatch in $CsLiB_6O_{10}$ crystal by means of temperature-profile compensation, Opt. Lett. **23**(13), 1016–1018 (1998).

[24] H. Kouta, Y. Kuwano, Attaining 186-nm light generation in cooled β-BaB_2O_4 crystal, Opt. Lett. **24**(17), 1230–1232 (1999).

[25] A. M. Roszkowska, G. Korn, M. Lenzner, M. Kirsch, O. Kittelmann, R. Zatonski, P. Ferreri, G. Ferreri, Experimental and clinical investigation of efficiency and ablation profiles of new solid-state deep-ultraviolet laser for vision correction, J. Cataract Refract. Surg. **30**(12), 2536–2542 (2004).

[26] I. Anderson, D. R. Sanders, P. van Saarloos, W. J. Ardrey IV, Treatment of irregular astigmatism with a 213 nm solid-state, diode-pumped neodymium: YAG ablative laser, J. Cataract Refract. Surg. **30**(10), 2145–2151 (2004).

[27] N. S. Tsiklis, G. D. Kymionis, G. A. Kounis, A. I. Pallikaris, V. F. Diakonis, S. Charisis, M. M. Markomanolakis, I. G. Pallikaris, One-year results of photorefractive keratectomy and laser *in situ* keratomileusis for myopia using a 213 nm wavelength solid-state laser, J. Cataract Refract. Surg. **33**(6), 971–977 (2007).

[28] A. M. Roszkowska, L. De Grazia, P. Ferreri, G. Ferreri, One-year clinical results of photorefractive keratectomy with a solid-state laser for refractive surgery, J. Refract. Surg. **22**(6), 611 (2006).

[29] N. S. Tsiklis, G. D. Kymionis, G. A. Kounis, I. I. Naoumidi, I. G. Pallikaris, Photorefractive keratectomy using solid state laser 213 nm and

excimer laser 193 nm: A randomized, contralateral, comparative, experimental study, Invest. Ophthalmol. Vis. Sci. **49**(4), 1415–1420 (2008).

[30] www.katanalaser.com, accessed on 2015-06-15.

[31] P. P. Van Saarloos, J. Rodger, Histological changes and unscheduled DNA synthesis in the rabbit cornea following 213-nm, 193-nm, and 266-nm irradiation, J. Refract. Surg. **23**(5), 477–481 (2007).

[32] M. H. Niemz, *Laser-Tissue Interactions: Fundamentals and Applications* (Springer, Berlin Heidelberg, 2007).

[33] R. W. Waynant, *Lasers in Medicine* (CRC press, Boca Raton, 2001).

[34] S. L. Trokel, R. Srinivasan, B. Braren, Excimer laser surgery of the cornea, Am. J. Ophthalmol. **96**(6), 710–715 (1983).

[35] A. Sugar, C. J. Rapuano, W. W. Culbertson, D. Huang, G. A. Varley, P. J. Agapitos, V. P. de Luise, D. D. Koch, Laser *in situ* keratomileusis for myopia and astigmatism: Safety and efficacy: A report by the American Academy of Ophthalmology, Ophthalmology **109**(1), 175–187 (2002).

[36] R. Ambrósio, S. E. Wilson, LASIK vs LASEK vs PRK: Advantages and indications, Semin. Ophthalmol. **18**(1), 2–10 (2003).

[37] G. L. Sutton, P. Kim, Laser *in situ* keratomileusis in 2010–A review, Clin. Experiment. Ophthalmol. **38**(2), 192–210 (2010).

[38] L. J. Kugler, M. X. Wang, Lasers in refractive surgery: History, present, and future, Appl. Opt. **49**(25), F1–F9 (2010).

[39] W. Sekundo, K. Kunert, C. Russmann, A. Gille, W. Bissmann, G. Stobrawa, M. Sticker, M. Bischoff, M. Blum, First efficacy and safety study of femtosecond lenticule extraction for the correction of myopia: Six-month results, J. Cataract Refract. Surg. **34**(9), 1513–1520 (2008).

[40] A. Dragomir, J. G. McInerney, D. N. Nikogosyan, Femtosecond measurements of two-photon absorption coefficients at λ=264 nm in glasses, crystals, and liquids, Appl. Opt. **41**(21), 4365–4376 (2002).

[41] L. I. Isaenko, A. Dragomir, J. G. McInerney, D. N. Nikogosyan, Anisotropy of two-photon absorption in BBO at 264 nm, Opt. Commun. **198**(4), 433–438 (2001).

[42] M. Divall, K. Osvay, G. Kurdi, E. Divall, J. Klebniczki, J. Bohus, Á. Péter, K. Polgár, Two-photon-absorption of frequency converter crystals at 248 nm, Appl. Phys. B **81**(8), 1123–1126 (2005).

[43] D. N. Nikogosyan, *Nonlinear Optical Crystals: A Complete Survey* (Springer, New York, 2005).

[44] J. C. Lagarias, J. A. Reeds, M. H. Wright, P. E. Wright, Convergence properties of the Nelder–Mead simplex method in low dimensions, SIAM J. Optim. **9**(1), 112–147 (1998).

[45] M. Vengris, E. Gabryte, A. Aleknavicius, M. Barkauskas, O. Ruksenas, A. Vaiceliunaite, R. Danielius, Corneal shaping and ablation of transparent media by femtosecond pulses in deep ultraviolet range, J. Cataract Refract. Surg. **36**(9), 1579–1587 (2010).

[46] E. Danieliene, E. Gabryte, R. Danielius, M. Vengris, A. Vaiceliunaite, V. Morkunas, O. Ruksenas, Corneal stromal ablation with femtosecond ultraviolet pulses in rabbits, J. Cataract Refract. Surg. **39**(2), 258–267 (2013).

[47] S. Tuft, R. Al-Dhahir, P. Dyer, Z. Zhu, Characterization of the fluorescence spectra produced by excimer laser irradiation of the cornea, Invest. Ophthalmol. Vis. Sci. **31**(8), 1512–1518 (1990).

[48] H. F. Li, W. M. Petroll, T. Møller-Pedersen, J. K. Maurer, H. D. Cavanagh, J. V. Jester, Epithelial and corneal thickness measurements by *in vivo* confocal microscopy through focusing (CMTF), Curr. Eye Res. **16**(3), 214–221 (1997).

[49] J. V. Jester, H.-F. Li, W. M. Petroll, R. D. Parker, H. D. Cavanagh, G. J. Carr, B. Smith, J. K. Maurer, Area and depth of surfactant-induced corneal injury correlates with cell death, Invest. Ophthalmol. Vis. Sci. **39**(6), 922–936 (1998).

[50] B. Masters, Three-dimensional confocal microscopy of the living *in situ* rabbit cornea, Opt. Express **3**(9), 351–355 (1998).

[51] W. M. Petroll, M. Weaver, S. Vaidya, J. P. McCulley, H. D. Cavanagh, Quantitative 3-dimensional corneal imaging *in vivo* using a modified HRT-RCM confocal microscope, Cornea **32**(4), e36–e43 (2013).

[52] B. J. Reiser, T. S. Ignacio, Y. Wang, M. Taban, J. M. Graff, P. Sweet, Z. Chen, R. S. Chuck, In vitro measurement of rabbit corneal epithelial

thickness using ultrahigh resolution optical coherence tomography, Vet. Ophthalmol. **8**(2), 85–88 (2005).

[53] C. Rathjen, W. Zesch, M. Deyerler, H. Lubatschowski, T. Ripken, Ophthalmologic device for breaking down eye tissue, US Patent App. 11/449,626 (2007).

[54] D. Brooks, N. Brown, D. Savage, C. Wang, W. Knox, J. Ellis, Precision large field scanning system for high numerical aperture lenses and application to femtosecond micromachining of ophthalmic materials, Rev. Sci. Instrum. **85**(6), 065107 (2014).

[55] M. Miclea, U. Skrzypczak, S. Faust, F. Fankhauser, H. Graener, G. Seifert, Nonlinear refractive index of porcine cornea studied by z-scan and self-focusing during femtosecond laser processing, Opt. Express **18**(4), 3700–3707 (2010).

[56] J. Pepose, H. Lubatschowski, Comparing femtosecond lasers, Cataract Refract. Surg. Today **10**, 45–52 (2008).

[57] A. Issa, U. Al Hassany, Femtosecond laser flap parameters and visual outcomes in laser *in situ* keratomileusis, J. Cataract Refract. Surg. **37**(4), 665–674 (2011).

[58] S.-M. Saw, G. Gazzard, E. C. Shih-Yen, W.-H. Chua, Myopia and associated pathological complications, Ophthalmic Physiol. Opt. **25**(5), 381–391 (2005).

[59] I. Ratkay-Traub, T. Juhasz, C. Horvath, C. Suarez, K. Kiss, I. Ferincz, R. Kurtz, Ultra-short pulse (femtosecond) laser surgery: Initial use in LASIK flap creation, Ophthalmol. Clin. North. Am. **14**(2), 347–55 (2001).

[60] P. S. Binder, Flap dimensions created with the IntraLase FS laser, J. Cataract Refract. Surg. **30**(1), 26–32 (2004).

[61] S. Wu, G. A. Blake, S. Sun, J. Ling, A multicrystal harmonic generator that compensates for thermally induced phase mismatch, Opt. Commun. **173**(1), 371–376 (2000).

[62] T. Seiler, G. Kahle, M. Kriegerowski, Excimer laser (193 nm) myopic keratomileusis in sighted and blind human eyes, Refract. Corneal Surg. **6**(3), 165–173 (1989).